LBL--24212

DE89 013366

LBL-24212

APPLIED SCIENCE DIVISION ANNUAL REPORT

ENVIRONMENTAL RESEARCH PROGRAM

FY 1987

Elton J. Cairns
Head, Applied Science Division
and
Associate Director, LBL

Tihomir Novakov
Program Leader, Environmental Research Program

Applied Science Division
Lawrence Berkeley Laboratory
University of California
Berkeley, California 94720

Prepared for the U.S. Department of Energy under Contract No. DE-AC03-76SF00098

CONTENTS

COMBUSTION RESEARCH

MEMBRANE BIOENERGETICS

ANALYTICAL CHEMISTRY

ENVIRONMENTAL RESEARCH PROGRAM STAFF

Tihomir Novakov, Program Leader
Nancy Brown, Deputy Program Leader

ATMOSPHERIC AEROSOL RESEARCH

Henry Benner
Fernando Diaz*
Raymond Dod
Lara Gundel
Anthony Hansen
Samuel Markowitz
Tihomir Novakov†
Roland Otto
Wanda Reyes*
Richard Schmidt
Nicole Somorjai
Su Wei-Han*
Linda Wroth

FLUE GAS CHEMISTRY

Shih-Ger Chang†
Ke-Yuan Hu*
David Littlejohn
David Liu
Allene Johnson

COMBUSTION RESEARCH

James Bonini
Nancy Brown†
John Cavolowsky
Robert Cheng
Peck Cho‡
Mariah Cochrane
John Dailey
Cheryl Ehorn
David Faris
Charles Fleischman
Erica Fono
Stephanie Frolich
Iskander Gokalp*
Ralph Greif
Jean Hertzberg
Kenneth Hom
Wei-Ming Huang
Gary Hubbard
Frank Hurlbut
Chung Lau‡
Donald Lucas
Richard Martin
Andrew Maxson
Fred Mowrer
Antoni Oppenheim
Ahmed Rashed
Chang Woo Rhee
Frank Robben
Douglas Rotman
Robert Sawyer
Frank Schipperijn
Ian Shepherd§
Pauline Sherman
Horton Stewart§
Lawrence Talbot
Eric Wakahiro
R. Brady Williamson

MEMBRANE BIOENERGETICS

Charles Blanchard
Ian Fry
John Harte
Eva Robinson
Margaret Huflejt
Johanna Lang
John Maguire
Rolf Mehlhorn
Harvey Michaels
Lester Packer†
Richard Schneider

ANALYTICAL CHEMISTRY

Frank Asaro†
Robert Glauque
Helen Michel
Amos Newton
Linda Sindelar
Fred Stross*
Isadore Perlman
Kristine Ing

ADMINISTRATIVE SUPPORT

Gloria Gill
Patti Hannah
Eric Essman

*Participating guest, †Group Leader, ‡University of California Davis,
§University of California Berkeley.

ENVIRONMENTAL RESEARCH PROGRAM

INTRODUCTION

The principal objective of the Environmental Research Program is to understand the formation, transformation, transport, and effects of energy-related pollutants on the environment, and how these are influenced by energy generation and emission control technology. Because a comprehensive understanding of these processes is crucially dependent on experimental data, a substantial effort in the Program is devoted to development and application of state-of-the-art measurement and analytical methods. This multidisciplinary research program includes fundamental and applied research in physics, chemistry, engineering, and biology, as well as research on the development of advanced methods of measurement and analysis. The Program's Annual Report contains summaries of research performed during FY 1987 in the areas of atmospheric aerosols, flue gas chemistry, combustion, membrane bioenergetics, and analytical chemistry.

The main research interests of the Atmospheric Aerosol Research Group concern the chemical and physical processes that occur in haze, clouds, and fogs. For their studies, the group is developing novel analytical and research methods for characterizing aerosol species. Aerosol research is performed in the laboratory and in the field. Studies of smoke emissions from fires and their possible effects on climatic change, especially as related to nuclear winter, are an example of the collaboration between the Atmospheric Aerosol Research and Combustion Research Groups.

The Flue Gas Chemistry Research Group is engaged in research whose aim is to help develop new processes for simultaneous SO_2 and NO_x removal. Current research is directed toward understanding the kinetics and mechanisms of homogeneous and heterogeneous catalysis of the interactions of sulfur dioxide and nitrogen oxides, both among themselves and with other compounds. When this fundamental chemistry is understood, it will be applied to the development of an efficient, cost-effective scrubber for simultaneous desulfurization and denitrification of flue gases.

The Combustion Research Group studies complex combustion processes by acquiring a fundamental understanding of the physical and chemical processes that determine the combustion efficiency, formation, and emissions of species from these processes. Controlled combustion studies have a goal of developing means whereby the zone of chemical activity would be spread out, so that its distribution in space and time could be controlled. The characterization and understanding of turbulence and its relationship to the combustion process are studied in simplified laboratory-scale burners using advanced laser diagnostic techniques. Combustion chemistry studies center on the theoretical understanding of thermal and state-to-state reactions with the purpose of characterizing elementary reactions and developing predictive capabilities.

The Membrane Bioenergetics Group studies the effects ofof strongly chemically reactive compounds generated within cells. Specific research efforts in FY 1987 were in photochemical conversion of solar energy by microbial systems. They are currently investigating biological oxidation and bioenergetics of cyanobacteria, bacteriorhodopsin, and bacterial succinate dehydrogenase. Another area of the Group's interest is in development and application of new assays of oxidation damage by using free radical measurements that arise during normal metabolism and under pathological conditions.

One of the main emphases in Analytical Chemistry has continued to be in the area of asteroid impacts and mass extinctions. The nature of the sedimentation of the rocks, the worldwide extent of the extinction horizons, and the extent to which the extinctions are related to impacts are also studied. Another area of emphasis is the application of synchrotron radiation to the analysis of minute amounts of trace elements in a variety of environmental and other samples.

The short reports that follow describe the program activities in FY 1987. For many of these reports, more detailed papers have been or will be published in appropriate scientific journals.

Incorporation of Soot Particles into Droplets*

W.H. Benner, A.D.A. Hansen, and T. Novakov

The incorporation of particles into fog or cloud droplets is influenced by factors such as particle size, composition, and the supersaturation of water vapor. For soot particles, their size and composition are affected by combustion conditions and fuel composition. Because fossil fuels contain differing amounts of sulfur, some of which is converted into particulate sulfate during combustion, its concentration in the fuel critically affects the nucleation properties of soot particles. Using a previously described chamber,[1] we have continued to study the influence of fuel sulfur on soot particle composition and on the nucleation of soot particles. By introducing SO_2 and NH_3 into the soot particle-droplet reaction system, we have also been able to study the influence of heterogeneous sulfate formation.

ACCOMPLISHMENTS DURING FY 1987

A two-channel aethalometer[2] has been used to determine the total and interstitial concentrations of black carbon in the fog chamber as a function of fuel sulfur content. In Fig. 1, the line drawn through the solid circles indicates the fraction of black carbon incorporated into droplets as a function of the total black carbon concentration for soot particles produced by the combustion of nearly sulfur-free propane. As the black carbon concentration increased, the fraction incorporated into droplets decreased because a fixed amount of water vapor that is available for droplet formation has to be distributed among the active nuclei. The line drawn through the boxes in Fig. 1 shows the incorporation of black carbon produced from propane fuel that contained 2.5% (wt/wt) sulfur. The fraction of black carbon incorporated into droplets also decreased as the black carbon concentration increased, but the effect of fuel

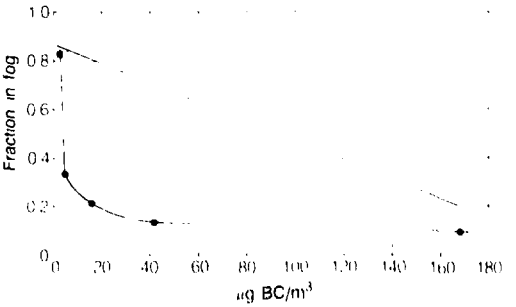

Figure 1. The effect of fuel sulfur on the incorporation of black carbon particles. The solid circles indicate the mass fraction incorporated into droplets for nearly sulfur-free propane combustion particles. For similar nucleation conditions, the boxes indicate that increased incorporation occurs for soot particles produced by the combustion of propane containing 2.5% (wt/wt) sulfur. (XBL 882-8362)

sulfur is obvious. The cause for the increased incorporation is an increase in the particulate sulfate/black carbon ratio that occurred with enrichment in fuel sulfur. The results led us to hypothesize that soot particles from sulfur-rich fuels have shorter atmospheric lifetimes than soot particles from sulfur-poor fuels.

Studies were conducted in which the concentration of particulate sulfate in the chamber was measured as a function of $[NH_3]$, $[SO_2]$, and black carbon concentration. The presence of NH_3 in this heterogeneous reaction system significantly increased the formation of particulate sulfate—a result that was not observed in the absence of droplets and/or soot particles. In the presence of droplets, the formation of particulate sulfate depended strongly on the black carbon concentration.

PLANNED ACTIVITIES FOR FY 1988

We plan to continue these studies so that the heterogeneous reactions of NH_3, SO_2, soot, and droplets in the atmosphere can be described kinetically.

*This work was supported by the Director, Office of Energy Research, Office of Health and Environmental Research, Physical and Technological Research Division of the U.S. Department of Energy under Contract No. DE-AC03-76SF00098, and by the National Science Foundation under Contract ATM 8713712.

REFERENCES

1. Benner, W.H., Hansen, A.D.A., and Novakov, T. (1987), *FY 1986 Annual Report of the Environmental Research Program*, Lawrence Berkeley Laboratory report LBL-22154, p. 4-7.
2. Hansen, A.D.A., Rosen, H., and Novakov, T. (1984), "The Aethalometer—An Instrument for the Real-Time Measurement of Optical Absorption by Aerosol Particles", *Sci. Total Environ. 36*, p. 191.

The Incorporation of Ambient Carbonaceous Aerosols in Advection Fog*

A.D.A. Hansen and T. Novakov

Aerosol black carbon is a ubiquitous pollutant species produced by incomplete combustion. In addition to impacts on visibility and the solar radiation balance, caused by its large optical absorption, it may also participate in heterogeneous-phase reactions of importance in atmospheric chemistry. The oxidation of SO_2 to sulfate in a water film on a carbon surface has been demonstrated in the laboratory. However, it was generally believed that ambient carbonaceous aerosols are hydrophobic, and therefore the contribution of this mechanism to aerosol acidification was of unknown significance. In this article we present the results of a field study showing that up to 80% of the ambient black carbon aerosol can be found incorporated into fog droplets.

ACCOMPLISHMENTS DURING FY 1987

To study the incorporation of aerosol black carbon into fogs, we used a two-channel aethalometer to measure this aerosol component in real time. One channel sampled the total aerosol through an open probe, heated to evaporate any fog water. This channel therefore measured both the interstitial aerosol and any black carbon that had been occluded by fog droplets. The other channel was preceded by several layers of nylon mesh, which served to impact any particles of aerodynamic diameter greater than 1 μm, and therefore to remove any droplets. This channel therefore measured only the interstitial aerosol. The presence of fog was detected semi-quantitatively by an infrared transmissometer.

This equipment was set up at U.C. Davis during January and February, 1987, to study radiation fogs common in winter in the central California valley. Unfortunately, an unsuitable location and abnormal winter meteorology resulted in very little fog being sampled. In August and September, 1987, the equipment was set up at LBL to study marine advection fogs common in the Bay Area in summertime. Figure 1 shows the incorporation of aerosol black carbon as a function of time during a fog impact; Fig. 2 shows the incorporation fraction vs. total black carbon concentration for 20-min data averages during both foggy and clear periods. It is clear that at low aerosol concentrations, a majority of the black carbon is indeed occluded by fog droplets. The transit times of these particles from the urban source regions to LBL were short ($\leq$ 1 hr), implying that this hygroscopicity is an attribute of the primary aerosol.

PLANNED ACTIVITIES FOR FY 1988

In collaboration with U.C. Davis, the equipment will be set up at a more suitable location in flat open terrain to study wintertime radiation fog in the central California valley.

*This work was supported by the National Oceanic and Atmospheric Administration under contract 40 RANR 520248, Coordinating Research Council, and the U.S. Department of Energy under Contract No. DE-AC03-76SF00098.

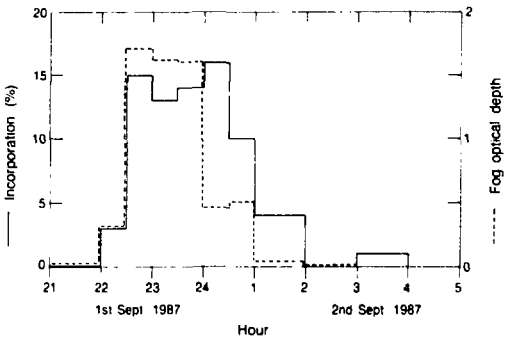

Figure 1. Fraction of ambient black carbon aerosol incorporated into fog droplets during marine advection fog episodes, plotted vs. total black carbon concentration. Each point represents a 20-min average of the continuous data for sampling times during a 7-day interval. Data for both foggy and clear periods are shown. (XBL 881-9625)

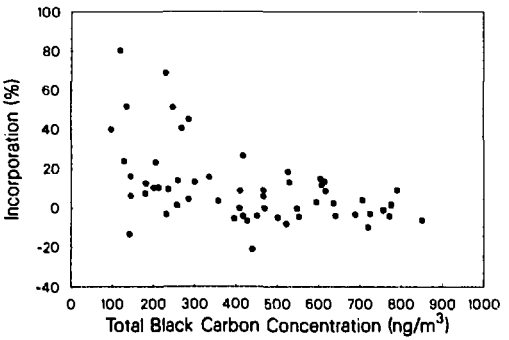

Figure 2. Fraction of ambient black carbon aerosol of size smaller than 0.3 μm, relative to total concentration. Data averaged by hour (local time) for 27 days in June and July at Claremont College, California (1987 summer SCAQS program). (XBL 879-11386)

Development of Real-Time Measurement Capability for Particulate Ammonium, Sulfate, and Nitrate*

L.A. Gundel and T. Novakov

The inorganic ions ammonium, sulfate, and nitrate are among the principal components of atmospheric particles. To begin to develop real-time measurement capability for these species, ambient particles were collected on Teflon filters while their absorbance was continuously measured, using Fourier transform infrared spectroscopy. Measurements of concentrations of NH_4^+, $SO_4^=$, and NO_3^- are currently performed routinely by ion chromatographic analyses of water extracts of filter samples of particles. Besides involving time-consuming sample preparation steps, this destructive technique may not actually reflect the original composition of the particles because of subsequent chemical changes on the filters. Another drawback of extraction-based analytical methods is the limit of detection. For $SO_4^=$, ion chromatography requires sampling times of at least 4 hr to obtain loadings > 1 $\mu g/cm^2$ on the filter.

*This work was supported by the Director, Office of Energy Research, Office of Health and Environmental Research, Physical and Technological Research Division of the U.S. Department of Energy, under Contract No. DE-AC03-76SF00098, and by the National Science Foundation under Contract No. ATM 8713712.

ACCOMPLISHMENTS DURING FY 1987

Figure 1 shows infrared absorbance due to NH_4^+, $SO_4^=$, and water for particles collected from ambient room air after 20 min of sampling. Using a sampling

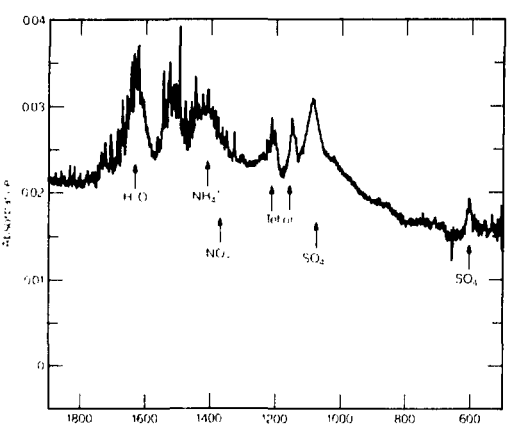

Figure 1. Infrared absorbance of ambient indoor particles, collected on a Teflon filter after 20 min of sampling. (XBL 882-11001)

rate of 20 liters/min and a collection area of 1 cm^2, the nondestructive FTIR technique detected $SO_4^=$ at $\leq 0.05\ \mu g/cm^2$ with a sampling time of 10 min or less. This is at least 20 times more sensitive for $SO_4^=$ than ion chromatography.

PLANNED ACTIVITIES FOR FY 1988

Measurements of the sensitivity of the method for NH_4^+ and NO_3^- will be made. The technique will be used to monitor particulate NH_4^+, $SO_4^=$, and NO_3^- indoors and outdoors.

The Interaction of NO_2 with Carbon Particles*

L.A. Gundel and T. Novakov

Both nitrous and nitric acids are found in polluted air. Nitric acid is an important component of acid deposition; nitrous acid may be a health hazard and pathways for its production in the atmosphere here have not yet been identified. This work explores the potential for carbon particles to play a role in heterogeneous production of NO_2^- and NO_3^- in the atmosphere and in indoor environments.

ACCOMPLISHMENTS DURING FY 1987

The interaction of NO_2 in air (0.5-35 ppm) with 20-mg carbon particles led to three products: NO, detected in the gas phase, and NO_2^- and NO_3^-, removed from the particles by water extraction. Figure 1 shows that the relative amounts of these products depended on the NO_2 concentration and the presence of water. At 4 ppm or below, in dry or humid air, the product distribution, in relative molar amounts, was $NO_3^- = 2NO_2^- = 2NO$. At 20 ppm and above, the relative amounts of products depended on the presence of water vapor: in dry air $NO = 3NO_3^- = 6NO_2^-$; in humid air $NO = NO_2^- = 2NO_3^-$. For carbon slurries in water, $[NO_2^-] = 6[NO_2^-]$ at an input concentration of NO_2 of 4 ppm. In comparison to carbon, alumina particles and glass beads removed NO_2 ineffectively. At 4 ppm carbon removed 97%, while alumina and glass removed 8 and 0% of the input NO_2 respectively.

These results indicate that NO_2 oxidized the carbon particles while it was reduced to NO. NO_2 adsorbed at oxidized sites on the particles formed a

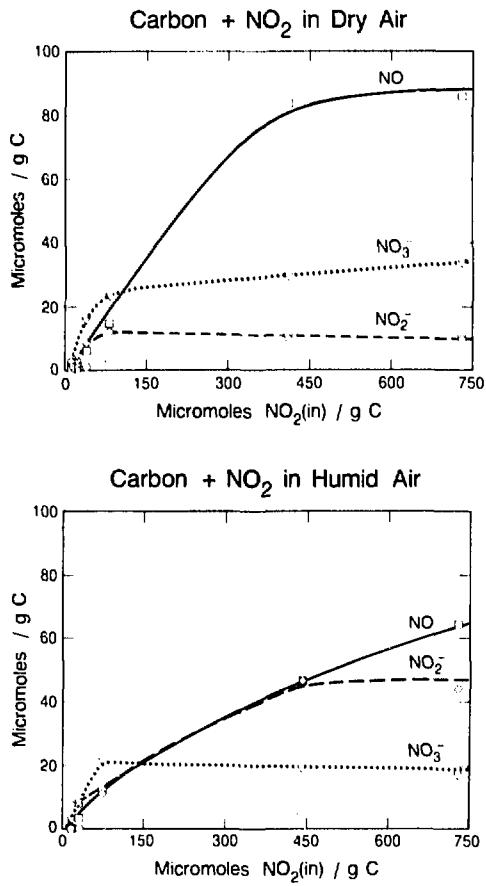

Figure 1. Amounts of nitrogenous species resulting from the interaction of NO_2. Upper: NO_2 in dry air; lower: NO_2 in humid air (50% relative humidity). Hexagons represent NO_2 measured downstream of the reaction vessel. (XBL 881-8806A)

*This work was supported by the Director, Office of Energy Research, Office of Health and Environmental Research, Physical and Technological Research Division of the U.S. Department of Energy, under Contract No. DE-AC03-76SF00098, and by the National Science Foundation under Contract No. ATM 8713712.

surface species that was analyzed as nitrate. When NO_2 adsorbed at other (nonoxidized) sites, equal amounts of NO_2^- and NO_3^- formed, as expected from reactive dissolution behavior of NO_2. At high enough concentrations of NO_2 (20 ppm and above), the interaction of NO with the surface nitrate produced NO_2^-. In slurries, NO, generated from interaction of NO_2 with carbon, reacted with surface nitrate or nitric acid in solution to form the relatively large quantities of nitrite observed here. This work suggests that NO_x reactions with carbon in droplets or on wet surfaces could be important sources for the production of nitrous acid in the environment; on dry particles both nitrous and nitric acids could be formed by this pathway.

PLANNED ACTIVITIES FOR FY 1988

We plan to continue this work with carbon, combustion soot, urban particulate matter, and slurries of typical fog water composition. The rates of production of NO, NO_2^-, and NO_3^- will also be measured.

Smoke Emissions from Medium-Scale Oil Pool Fires*

R.L. Dod, R.B. Williamson, N.J. Brown, and T. Novakov

Evaluation of the potential significance of a "nuclear winter" produced by smoke from post-nuclear exchange fires depends largely upon the quantity of smoke generated, its distribution in the atmosphere, and its optical characteristics.[1] Existing information regarding these factors is insufficient to reliably estimate the effects of such fires.[2] It is considered that smoke contributions from burning of petroleum stocks may be a major contributor to the climatic effects due to fuel concentration and smoke emissions factors. We have extended our previous measurements of emission factors and size distributions for smoke from burning urban building materials[3] to include emissions from fuel oil pool fires under both free-burning and ventilation-restricted conditions.

ACCOMPLISHMENTS DURING FY 1987

The series of experiments conducted this year were primarily with fuel oil pool fires. Both fire scale and ventilation conditions were varied to produce a data set from which extrapolation to large-scale fires could be reasonably done. The oil was burned in pools 56 cm in diameter, either individually or in two similar pools side by side. Single 56-cm pools were also burned in the "burn room," a fire-resistant, enclosed room at the University of California's Fire Research Laboratory.

Average measured emission factors (smoke particle mass as a fraction of fuel consumed) are shown in Fig. 1, together with those for building materials determined previously. The smoke generated from burning single pans of oil exceeded 10% of the consumed fuel mass, a fraction that is in general agreement with that from burning asphalt roofing. When the fire intensity was increased by burning two pools

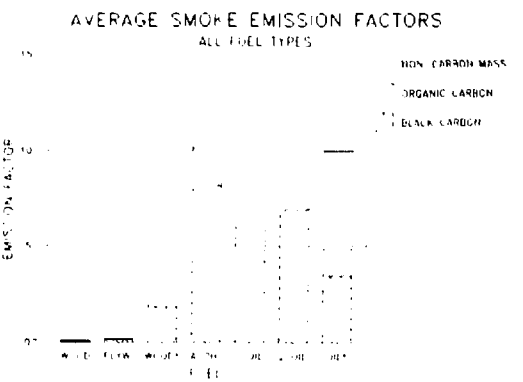

Figure 1. Measured average emission factors for all fuel types. WOOD refers to solid wood, PLYW, to plywood, and ASPH, to asphalt roofing shingles. WOOD* and OIL* refer to fuels burned under restricted ventilation conditions. (XBL 882-546)

*This work was supported by the Defense Nuclear Agency through the U.S. Department of Energy under Contract No. DE-AC03-76SF00098.

of oil side by side, smoke emissions dropped by a reproducible amount. Whether this change will hold with further increase in scale or change of configuration is not known. Soot carbon emissions from oil burned under ventilation restricted conditions were approximately 50% less than was observed for similar scale fires in the open. (The large non-carbon smoke mass in these experiments is probably from the lining of the burn room or the antechamber, which was also involved in fire from pyrolyzates during flashover.) We do not know why there is a decrease in emission factor when oil is burned under limited ventilation conditions, while wood burned in a similar fashion shows a dramatic increase in emissions.

Particle size distributions for the fires in the open showed the largest fraction to be less than 0.3 μm aerodynamic diameter, although a secondary peak was apparent in the distribution functions at 1-2 μm. As with underventilated wood fires, the particle mass peak shifted into the 1-2 μm range, with few fine particles present. This shift in particle size is potentially important to the prediction of climatic effects, since Penner[4] has calculated that particles >1 μm diameter are much more susceptible to incorporation into water droplets and thus potentially to rainout than are particles in the 0.1 to 0.3 μm size range.

PLANNED ACTIVITIES FOR FY 1988

We intend to continue this work with further exploration of the effects of scaling, fuel geometry, and composition to the extent that our facility will allow.

REFERENCES

1. Turco, R.P., Toon, O.B., Ackerman, T.P., Pollack, J.B., and Sagan, C. (1983), "Nuclear Winter: Global Consequences of Multiple Nuclear Explosions," *Science* 222, p. 1283.
2. National Research Council, Committee on the Atmospheric Effects of Nuclear Explosions, Commission on Physical Sciences, Mathematics and Resources (1985), *The Effects on the Atmosphere of a Major Nuclear Exchange*, National Academy, Washington.
3. Dod, R.L., Brown, N.J., Mowrer, F.W., Novakov, T., and Williamson, R.B. (1988), "Smoke Emission Factors from Medium Scale Fires: Part 2", submitted to *Aerosol Sci and Technol.*
4. Penner, J.E., "Predicting the Consequences of Nuclear War," *3rd International Conference on Carbonaceous Particles in the Atmosphere*, October 3-8, 1987, Berkeley, California.

Single Submicron-Sized Particle Analysis*

W.H. Benner and R. Otto

Currently available information on the composition of individual submicron particles is extremely limited. This information is useful because currently available techniques provide composition data that can only be reported as an average of all particles, even though individual particles in a sample can have greatly differing compositions. Particle analysis in real time will provide additional benefits, one of which is the preclusion of particle contamination (artifact formation) during sample collection time.

*This work was supported by the Director, Office of Energy Research, Office of Health and Environmental Research, Physical and Technological Research Division of the U.S. Department of Energy under Contract No. DE-AC03-76SF00098.

ACCOMPLISHMENTS DURING FY 1987

We have started a new project in which a method to analyze individual particles in real time for elemental composition is being developed. Particles in the diameter range of 0.01 to 10 μm will be electrically charged and accelerated to velocities such that their impact with a target will produce a plasma. The plasma will be analyzed by mass spectrometry for elements.

Charged test particles of activated carbon, polystyrene spheres, sodium chloride, and fluorescent dyes were generated and drawn into a sonic velocity accelerator (Fig. 1). This differentially pumped capillary-skimmer system was built and tested as a way to produce a well-defined beam of particles in vacuum and is to be used eventually to inject particles into a 100-kv electrostatic accelerator. Performance tests showed that as the particle beam exited the skimmer, it diverged only 0.2°. The velocity of the particles in the beam was measured by use of

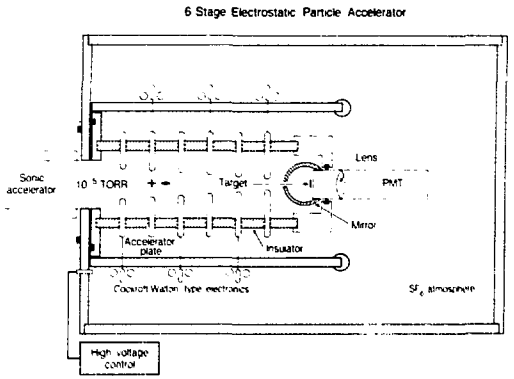

Figure 1. Schematic of a sonic velocity accelerator in which a capillary-skimmer system is used to produce a beam of test particles in vacuum. (XBL 881-8337)

two rotating disks. A hole in the first disk chopped the beam; and the second disk, spaced 8.5 cm from the first, was used to collect particles by impaction. Measurement of the disks' rotational speed and the angular displacement of the beam spot from a center line position on the second disk showed particle velocity to be ~ 300 m/sec or ~ 95% of sonic velocity. This particle velocity indicated that the differentially pumped capillary skimmer was working without fluid flow disturbances and will provide a way to inject electrically charged particles into an electrostatic accelerator that is currently under construction.

PLANNED ACTIVITIES FOR FY 1988

We plan to continue to develop this analytical technique. The sonic accelerator will be coupled to a 100-kv electrostatic accelerator, and we will attempt to detect high velocity particle impact events.

Reaction of Nitric Oxide with Fe(II) Complexes of SH-Containing Amino Acids*

D.K. Liu, D. Littlejohn and S.G. Chang

Conventional ferrous chelates employed in wet flue gas scrubbing systems to promote NO removal include Fe^{2+}(EDTA) and Fe^{2+}(NTA). We recently reported a process using ferrous cysteine as additive which possesses several advantages over the conventional Fe^{2+}(EDTA)-type chelates.[1] We have since extended our effort to include ferrous chelates of other SH-containing amino acids and peptides.

ACCOMPLISHMENTS DURING FY 1987

We have discovered that ferrous chelates of N-acetylcysteine (AcCySH), penicillamine (Pen), N-acetylpenicillamine (AcPen), glutathione (GSH), and cysteinylglycine (cys-gly) are more effective in NO removal compared to that of cysteine (CySH).[2] The experiments were carried out at 55°C and between pH 4.3 and 12.0 by bubbling a gaseous mixture of NO(P_{NO} = 500 ppm), O_2 (4%) and N_2 (balance) into an absorber containing a buffered solution of ferrous salt (0.01 M) and amino acid/peptide (0.04 M). The results are shown in Figure 1. While the NO absorption capacity of $Fe^{2+}(CyS)_2$ is fairly insensitive to pH, $Fe^{2+}(Pen)_2$, $Fe^{2+}(AcCyS)_2$, and $Fe^{2+}(AcPen)_2$ are most efficient in neutral solutions (pH ~ 7) and become ineffective in acidic (pH < 6) or strongly alkaline (pH > 11) medium. The ferrous peptide complexes behave somewhat differently from the amino acid complexes. The maximum NO removal capacity for Fe^{2+}(GS) was found at pH 5.4, with nNO/nFe^{2+} = 0.54. The Fe^{2+}(cys-gly)$_2$ system absorbed NO under all conditions studied. The nNO/nFe^{2+} ratio was 0.28 between pH 4.3 and 5.5, rose to 0.87 at pH 7.3, and then dropped off rapidly as the pH increased, falling to 0.05 at pH 9.2.

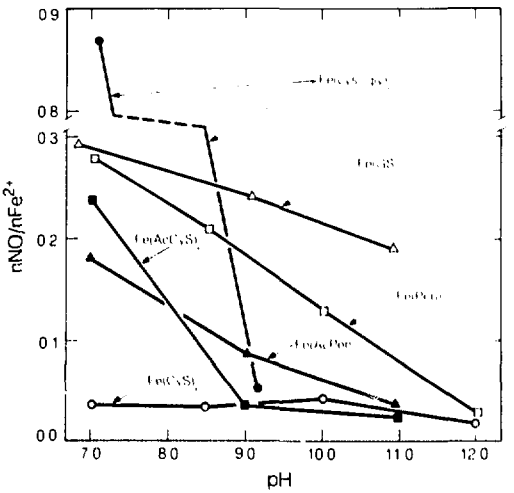

Figure 1. The NO absorption capacity of ferrous thioamino acid/-peptide complexes as a function of pH. (XBL 8711-9339)

The fate of the absorbed NO was determined by vacuum line experiments at pH 7.0 in the absence of O_2. In the case of $Fe^{2+}(CyS)_2$, 46% of the absorbed NO was reduced to a ~ 1:1 mixture of N_2 and N_2O, with the remaining of the absorbed NO in a $Fe(CySSCy)(NO)_2$ precipitate. For $Fe^{2+}(Pen)_2$, all of the absorbed NO was reduced to N_2 (~ 91%) and N_2O (~ 9%) in the gas phase. In the Fe^{2+}(GS) system, all of the absorbed NO was converted to a mixture of NO_2^- (> 85%) and NO_3^- (5-15%) in solution. The different NO-derived products imply different mechanisms are involved in the ferrous amino acid and peptide systems. Finally, we have found that the disulfide forms of CySH, AcCySH and GSH obtained after NO absorption can be reduced back to the starting thiols using a simple and potentially cost-effective method involving $H_2S/SO_2/OH^-$. For the regeneration of thiols from the disulfides of Pen, AcPen and cys-gly, electrochemical reduction appears to be the only viable method at present.

PLANNED ACTIVITIES FOR FY 1988

The study of these systems has been completed and no further work is planned.

*This work was supported by the Assistant Secretary for Fossil Energy, Office of Coal Utilization Systems, U.S. Department of Energy under Contract No. DE-AC03-76SF00098 through the Pittsburgh Energy Technology Center, Pittsburgh, PA.

REFERENCES

1. Liu, D.K., Frick, L.P., and Chang, S.G. (1988), "A Ferrous Cysteine Based Recyclable Process for the Combined Removal of NO_x and SO_2 from Flue Gas ," *Environ. Sci. Technol.*, 1988, *22*, 000.

2. Chang, S.G., Littlejohn, D. and Liu, D.K. (1987), "Use of Ferrous Chelates of SH-Containing Amino Acids and Peptides for the Removal of NO_x and SO_2 from Flue Gas," submitted to *Ind. Eng. Chem. Res.*

Removal of Nitric Oxide from Flue Gas Using Water-Soluble Iron (II) Dithiocarbamates*

D.K. Liu and S.G. Chang

The reaction of metal dithiocarbamates with NO was first reported over fifty years ago. However, the metal dithiocarbamates and their nitrosyl complexes prepared thus far are predominantly those containing dialkyl substituents. These metal chelates are only soluble in organic solvents and therefore are not applicable to wet flue gas scrubbing systems in which water is the medium. Recently, it came to our attention that dithiocarbamates containing negatively charged carboxylate substitutents can be prepared by the reaction of glycine (Gly) and iminodiacetic acid (IDA) with carbon disulfide in sodium hydroxide solution. The iron (II) chelates of such dithiocarbamates should be water-soluble and therefore we decided to prepare these chelates and to study their reactions with NO.

ACCOMPLISHMENTS DURING FY 1987

We have prepared sodium N-carboxymethyl-dithiocarbamate via the reaction of Gly and CS_2 in 2.0 M sodium hydroxide solution as shown in equation 1.

$$HO_2CCH_2NH_2 + CS_2 + 2NaOH \rightarrow Na^+ \ O_2CCH_2NHCS_2 \ Na^+ + 2H_2O \quad (1)$$

Similarly, the reaction of IDA with CS_2 yields bis (N-carboxylmethyl) dithiocarbamate according to equation 2.

$$(HO_2CCH_2)_2NH + CS_2 + 3NaOH \rightarrow (Na^+ \ O_2CCH_2)_2NCS_2 \ Na^+ + 3H_2O \quad (2)$$

The presence of these dithiocarbamates derived from Gly and IDA (abbr. Gly-dtc and IDA-dtc, respectively) in the reaction mixture was confirmed by the precipitation of these intermediates as S-benzylthiuronate derivatives, and by uv-visible and laser Raman spectroscopies. Using the same method, dithiocarbamates derived from diethanolamine (DEA) and urea (abbr. DEA-dtc and urea-dtc, respectively) have also been prepared.

The removal of NO from a simulated flue gas mixture containing 500 ppm NO and 4% O_2 can be effected by aqueous solutions containing various iron

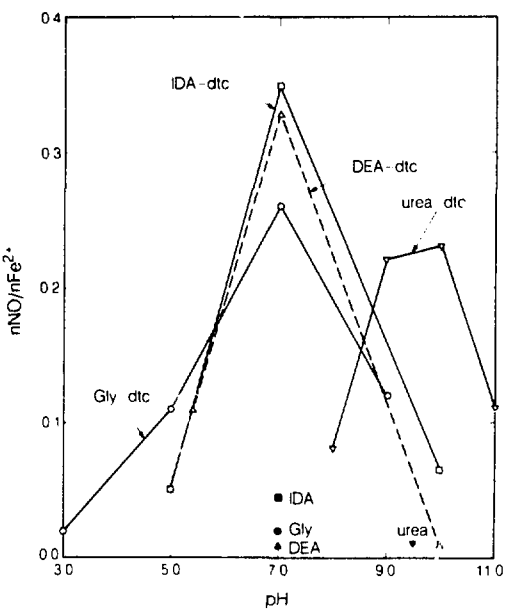

Figure 1. The NO absorption capacity of iron (II) dithiocarbamates as a function of pH. (XBL 8712-9111)

*This work was supported by the Assistant Secretary for Fossil Energy, Office of Coal Utilization Systems, U.S. Department of Energy under Contract No. DE-AC03-76SF00098 through the Pittsburgh Energy Technology Center, Pittsburgh, PA

(II) dithiocarbamates as shown in Figure 1. Most of the iron (II) dithiocarbamates in this study work best under neutral conditions, with the exception of Fe^{2+}(urea-dtc)$_2$, which is most effective between pH 9.0 and 10.0. Product analyses showed that most of NO absorbed by Fe^{2+}(Gly-dtc)$_2$ and Fe^{2+}(IDA-dtc)$_2$ solutions ended up as gas phase products N_2 and N_2O in ratios of ~ 4:1 and ~ 10:1, respectively.

PLANNED ACTIVITIES FOR FY 1988

Future efforts will be directed towards the isolation of pure alkali metal salts of the above dithiocarbamates for use in the absorbent solutions, complete characterization of the iron dithiocarbamates, and the extension of the present concept to xanthates and thioxanthates.

REFERENCES

1. Liu, D.K., and Chang, S.G. (1988), " Removal of Nitric Oxide from Flue Gas Using Water-Soluble Iron (II) Dithiocarbamates," submitted to *Ind. Eng. Chem. Res.*

Development of Reagents for Use in Spray-Drying Systems to Control SO_2 and NO_x Emissions*

D. Littlejohn and S.G. Chang

Of the emerging technologies for control of SO_2 and NO_x in flue gases, the spray-drying method has shown several economic and technical advantages over existing wet processes. To maximize the potential of a spray-drying desulfurization and denitrification system, reagents that effectively react with SO_2 and NO_x must be identified.

ACCOMPLISHMENTS DURING FY 1987

We have tested a number of compounds that are considered to have potential as spray-drying reagents in a bench-scale spray-drying system. A small spray dryer with a rotary atomizer to disperse the reagent solution into the hot flue gas was used. Simulated flue gas with about 500 ppm NO and about 2000 ppm SO_2 was heated and directed into the spray dryer. The test solution was fed into the atomizer. About 70% of the solid could be collected by a cyclone collector at the exit. A fraction of the gas leaving the system was directed into a chemiluminescent NO_x analyzer and a fluorescent SO_2 analyzer for measurement of the NO and SO_2 concentrations.

*This work was supported by the Assistant Secretary for Fossil Energy, Office of Coal Utilization Systems, U.S. Department of Energy under Contract No. DE-AC03-76SF00098 through the Pittsburgh Energy Technology Center, Pittsburgh, PA.

Two types of solutions were studied in the spray-drying system. One type of solution contained ferrous chelate complexes to bind NO and an alkaline compound to bind SO_2. The other type of solution contained oxidants to oxidize NO and SO_2 into nitrite/nitrate ion and sulfate ion. Runs were done at both room temperature at about 150°C. The gas flow rate was about 20 cfm.

EDTA, cysteine and cysteinylglycine were used as chelates in the ferrous chelate complex studies. Carbonate and/or bicarbonate salts were used as buffers. The chelates studied were chosen because they had worked well in bench-scale wet scrubbing systems. In the runs done with a gas inlet temperature of 25°C, cysteine had the highest removal of the chelates tested: 13%. EDTA and cysteinylglycine had lower removal rates. Some runs were done without oxygen, but no improvement in the NO removal rate was observed. The SO_2 removal was controlled by the amount of buffer present, and removal rates in excess of 90% could be achieved.

EDTA and cysteine were tested with a gas inlet temperature of about 150°C. As expected, the NO removal was less than that obtained at 25°C. Virtually no NO was removed with EDTA as a chelate, while NO removal was as high as 11% with cysteine as a chelate. Again, SO_2 removal in excess of 90% could be obtained. A test done by the Pittsburgh Energy Technology Center on ferrous cysteine in a similar system with a gas inlet temperature of 180°C obtained 24% NO removal and 96% SO_2 removal. From the results, it appears that ferrous chelate solutions are not well suited to spray-drying flue gas clean-up.

The second class of solutions studied, oxidants, had also showed promise in wet scrubbing NO_x and

SO_2 removal systems. The oxidants studied include H_2O_2, NaClO, $NaClO_2$, $NaClO_3$, $NaClO_4$, $Ca(ClO)_2$, $(NH_4)_2S_2O_8$ and $NaIO_4$. Most of these compounds were tested with gas containing NO, but not SO_2, since SO_2 can be readily removed by alkaline solutions. Of these compounds, $NaClO_2$ and NaClO proved to be the most promising. NaClO was influenced by the gas temperature significantly, and could remove up to about 20% of the NO. $NaClO_2$ worked well at 25°C, removing up to 75% of the NO, but its efficiency decreased with increasing temperature. It could remove less than 10% of the NO at 150°C.

PLANNED ACTIVITIES FOR FY 1988

There are many other possible compounds that may be useful in spray-drying systems. We plan to continue our search to identify effective and inexpensive compounds or mixtures of compounds for use in commercial spray-drying systems for SO_2 and NO_x control.

Removal of NO_x and SO_2 from Flue Gas by Treatment with Peroxyacids*

D. Littlejohn and S.G. Chang

Cost-effective and efficient methods are needed to simultaneously remove SO_2 and NO_x from flue gas effluent from coal-fired power plants. Metal-chelate based systems for simultaneous desulfurization and denitrification of flue gas show promise, but are generally sensitive to the oxygen in the flue gas. Use of oxidizing compounds as scrubbing agents would avoid the problem of oxygen sensitivity. One class of oxidizing compounds, peroxyacids (peracids), have been found to be particularly effective in removing NO_x and SO_2 from simulated flue gas.

ACCOMPLISHMENTS DURING FY 1987

Peroxyacids can be formed by mixing concentrated (30-70%) hydrogen peroxide with concentrated acid. The general reaction is:

$$X-OH + H_2O_2 \rightleftarrows X-OOH + H_2O$$

where an equilibrium exists between the peroxyacid and the acid. The peroxyacids which have been investigated so far are peroxysulfuric acid, peroxyformic acid and peroxyacetic acid. The ability of the peroxyacid solutions to remove NO and SO_2 from flue gas was studied in both a wet scrubbing system and a spray-drying system.

In the wet scrubbing system, the gas mixture containing NO and SO_2 was bubbled through a glass frit immersed in the peroxyacid solution. The gas mixture was then directed through a cold trap and to a chemiluminescent NO_x analyzer and a fluorescent SO_2 analyzer. The temperature of the scrubbing column containing the peroxyacid solution could be adjusted, if desired. NO concentrations of 360-550 ppm and SO_2 concentrations of 1400-2460 ppm were used in the experiments. A gas flow rate of 1 l/min was used with a scrubbing solution of 50 ml. The concentrations of the peroxyacids in the solution ranged from 1 to 4 M. The equilibrium constants for the acids differ and are temperature dependent. The temperature studied ranged from 25°C to about 55°C.

In all the wet scrubbing experiments where it was present, there was 100% removal of SO_2. Removal of NO was usually lower, although the removal of NO increased with increasing temperature. Runs done without SO_2 had better NO removal than runs done with SO_2. All three peroxyacids appeared to have similar abilities in NO and SO_2 removal. At 55°C, 90% NO removal and 100% SO_2 removal could be achieved.

In the spray-drying experiments, the gas mixture was heated to 110°C to 170°C before entering the chamber. The gas flow rate was about 600 l/min. The peroxyacid solution was fed into a rotary atomizer at a flow rate of 10 to 30 ml/min. The NO concentrations ranged from 550 to 850 ppm and the SO_2 concentrations ranged from 240 to 2740 ppm. The temperature of the gas leaving the spray-drying chamber ranged from 50°C to 95°C. In general, the amount of NO and SO_2 removed in spray-drying experiments were not as high as those achieved in the wet scrubbing experiments. The fraction of NO

*This work was supported by the Assistant Secretary for Fossil Energy, Office of Coal Utilization Systems, U.S. Department of Energy under Contract No. DE-AC03-76SF00098 through the Pittsburg Energy Technology Center, Pittsburgh, PA

removed ranged from approximately .04 to .41 and the fraction of SO_2 removed ranged from approximately zero to 1.00. Higher scrubbing solution feed rates increased the fraction of NO and SO_2 removed. Higher spray-drying temperatures increased NO removal but decreased SO_2 removal. The optimum conditions have not been determined.

PLANNED ACTIVITIES FOR FY 1988

We plan to continue studies of peroxyacids as flue gas scrubbing agents. The chemistry of the removal process and the reaction products will be investigated. The use of additives to improve removal rates in the spray-drying system will be attempted.

Disulfate Ion as an Intermediate in the Oxidation of Bisulfite Ion by O_2*

D. Littlejohn, K.Y. Hu and S.G. Chang

Most methods of removing SO_2 from flue gas involve the interaction of the gas with aqueous solutions. The SO_2 will readily dissolve in an aqueous solution, where its charge state will depend on the pH of the solution. The oxidation of the dissolved SO_2 is influenced by a number of factors, which must be understood to treat the scrubbing solution and remove the dissolved sulfur oxyanions.

ACCOMPLISHMENTS DURING FY 1987

Bisulfite ion (HSO_3^-) is the predominant form of dissolved SO_2 in the range of pH 2 to 7. The reaction of dissolved O_2 with HSO_3^- was studied using a high-pressure, rapid mixing flow system and a Raman spectrometer. By pressurizing the reaction system, the dissolved oxygen concentration could be raised to a level where it could be observed by Raman spectrometry. The reaction was studied by either collecting a Raman spectrum of mixed reactants while they flowed through the cell, or by observing the behavior of a Raman line of one compound when the flow was stopped.

In the studies of this reaction, an intermediate in the reaction was observed. From its behavior, we assigned $S_2O_7^{2-}$ as the formula for the intermediate. The intermediate hydrolyzes to form sulfate and hydrogen ion:

$$S_2O_7^{2-} + H_2O \rightarrow 2H^+ + 2SO_4^{2-}$$

From the hydrolysis rate constant and reaction products, and from the Raman spectrum, the intermediate has been identified as disulfate ion.[1] Sodium disulfate salt was prepared[2] and its Raman spectrum and hydrolysis rate was compared with those of the intermediate. The Raman spectra are shown in Fig. 1. Spectrum A is that of disulfate ion at 25°C. Data were collected in selected regions only because of its limited lifetime. Spectrum B is of disulfate ion at 0°C, where it is longer-lived. Spectrum C is the difference between freshly mixed and completed reacted $O_2 + HSO_3^-$. The two peaks at 1023 and 1055 cm^{-1} are due to HSO_3^-. The hydrolysis rate constant of the intermediate agrees very well with that of disulfate ion.[3]

PLANNED ACTIVITIES FOR FY 1988

The hydrolysis of disulfate ion is influenced by a number of metal cations.[3] We plan to study the influence of metal ions commonly found in scrubber

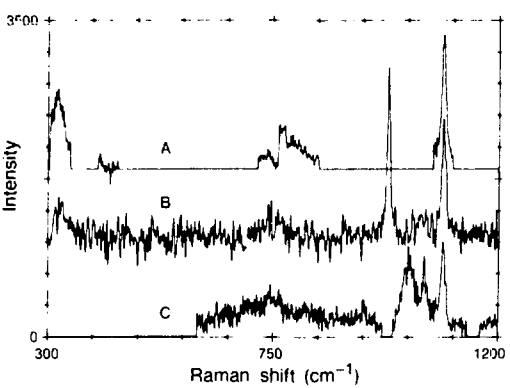

Figure 1. Raman spectra of A) disulfate ion at 25°C, B) disulfate ion at 0°C, and C) intermediate in reaction system. (XBL 8710-5923)

*This work was supported by the Assistant Secretary for Fossil Energy, Office of Coal Utilization Systems, U.S. Department of Energy under Contract No. DE-AC03-76SF00098 through the Pittsburgh Energy Technology Center, Pittsburgh, PA.

systems on the $S_2O_7^{2-}$ hydrolysis rate. Little is known about the formation of disulfate ion in the $O_2 + HSO_3^-$ reaction system. It is desirable to understand the mechanism by which it is formed.

REFERENCES

1. Chang, S.G., Littlejohn, D., and Hu, K.Y. (1987), "Disulfate Ion as an Intermediate to Sulfuric Acid in Acid Rain Formation," *Science 237*, p. 756.
2. Hofmeister, H.K., and Van Wazer, J.R. (1962), "Hydrolysis of Sodium Pyrosulfate," *Inorg. Chem. 1*, p. 811.
3. Thilo, E., and Von Lampe, F. (1963) "Beitrage zur Chemie der Alkalidi (=pyro) sulfate," *Z. anorg. allg. Chem. 319*, p. 387.

A Study of the Solubilities of Nitrogen-Sulfur Compounds*

D. Littlejohn, A. Johnson and S.G. Chang

The nitrogen-sulfur compounds hydroxyimidodisulfate (HIDS), hydroxysulfamate (HSA), nitridotrisulfate (NTS), and imidodisulfate (IDS) are formed by reactions of nitrite ion (NO_2^-) with bisulfite ion (HSO_3^-) in acidic or neutral solutions. Appreciable amounts of NO_2^- and HSO_3^- can form in some scrubbing systems designed to remove SO_2 and NO_x from flue gas. The solubilities of these nitrogen-sulfur compounds are needed, so that methods for removing them from scrubbing liquors can be developed.

ACCOMPLISHMENTS DURING FY 1987

The potassium salts of the nitrogen-sulfur compounds are among the least soluble of those with common cations. The potassium salts were prepared by methods given in the literature.[1,2,3] Saturated solutions of the salts were prepared by adding excess salt to water in a controlled-temperature bath. After allowing sufficient time for saturation to occur, the concentrations of the dissolved salts were determined. Two analytical methods were used. In the first method, a measured volume of the saturated solution was mixed with a measured volume of a sodium sulfate solution of known concentration. A Raman spectrum of the mixed solution was obtained, and the original concentration of the nitrogen-sulfur compound was calculated from the Raman peak heights.[4]

*This work was supported by the Assistant Secretary for Fossil Energy, Office of Coal Utilization Systems, U.S. Department of Energy under Contract No. DE-AC03-76SF00098 through the Pittsburg Energy Technology Center, Pittsburgh, PA.

In the second method, reference solutions of known concentrations were prepared for the nitrogen-sulfur compounds. Dilutions of the saturated solutions were prepared. For each compound, diluted samples and the reference solution were alternately injected into an ion chromatograph. The peak heights were then used to calculate the concentration of the saturated solution.[5]

Measurements were made on the potassium salts of HIDS, NTS and IDS. The measurements on IDS were complicated by the process:

$$IDS^{2-} \rightleftarrows IDS^{3-} + H^+ \qquad K_{a3} = 3.3 \times 10^{-9}$$

More work needs to be done under controlled pH conditions to obtain accurate data. For HIDS, the solubility as a function of temperature can be described as:

$$\text{solubility (moles/liter)} = 0.0106T(^\circ C) - .033$$

for a temperature range of 5 - 40°C. For NTS, the solubility equation is:

$$\text{solubility (moles/liter)} = 4.3 \times 10^{-4} T(^\circ C) + 2.9 \times 10^{-3}$$

over a temperature range of 5 - 65°C.

PLANNED ACTIVITIES FOR FY 1988

We plan to continue making solubility measurements on these compounds. Solubility of the two charge states of IDS are needed, as well as the solubility of HSA. It would be useful to have solubility data on all the compounds above 50°C.

REFERENCES

1. Sisler, H., and Audrieth, L.F. (1938), "Potassium Nitrilosulfonate," *J. Am. Chem. Soc. 60*, p. 1947.

2. Rollefson, G.K., and Oldershaw, C.F. (1932), "The Reduction of Nitrites to Hydroxylamine by Sulfites," *J. Am. Chem. Soc., 54*, p. 977.

3. Seel, V.F., and Degener, E. (1956), "Kinetik und Chemismus der Raschigschen Hydroxylamin-Synthese," *Z. anorg. allg. Chem., 284*, p. 101.

4. Littlejohn, D., and Chang, S.G. (1984), "Identification of Species in a Wet Flue Gas Desulfurization and Denitrification System by Laser Raman Spectroscopy," *Environ. Sci. & Tech., 18*, p. 305.

5. Littlejohn, D., and Chang, S.G. (1986), "Determination of Nitrogen-Sulfur compounds by Ion Chromatography," *Anal. Chem. 58*, p. 3131.

Controlled Combustion*

P.R. Breber, N.J. Brown, J.A. Cavolowsky, D.W. Faris, K. Hom, D. Lucas, J.A. Maxson, A.K. Oppenheim, D.A. Rotman, R.F. Sawyer and H.E. Stewart

The goal of this project is to provide scientific background for the development of controlled combustion engines. Their practical attributes consist of: 1° minimization of formation of pollutants, 2° optimization of the tolerance to a wide variety of fuels, and 3° maximization of fuel economy. In order to attain this, combustion chambers, considered so far as solely sources of power, have to be transformed into controlled chemical reactors. In principle this involves a fundamental modification of the combustion process so that, instead of having to rely upon a solitary flame, a single connected zone separating the burnt gas from the unburnt medium, it is accomplished by a multitude of flame kernels generated by exothermic ignition centers which are appropriately distributed throughout the working substance.[2,10,14] The best way to realize this is by the use of jets, capable of impregnating the combustible charge with controllable sets of ignition sources. Thus, the primary objective of experimental investigations was the exploration of the properties of pulsed jets, or puffs, of plasma, hot gas (flames), and liquid fuel (sprays), whereas, concomitantly, the fluid mechanical and thermochemical features of ignition and turbulent combustion fields and jets were at the focus of theoretical studies.

ACCOMPLISHMENTS DURING FY 1987

Pulsed Plasma Jets

Experimental investigation of the thermochemical and fluid mechanical properties of pulsed plasma jets was carried out by the use of, respectively, the molecular beam mass spectroscopy (MBMS) and the ultra-high frequency (~ MHz) schlieren cinematography. Last year, we developed a technique to calibrate the mass spectrometer for a quantitative determination of species concentrations. On this basis we measured concentration histories of such radicals as O, N and NO, produced by plasma jet igniters in nitrogen and air.[3] This led to the establishment of the MBMS technique for concentration measurements in combustible mixtures, applicable, in particular, to active radicals, such as CH_3, O, H, and OH, in lean hydrocarbon-air mixtures - a subject currently under study.[13] At the same time, the schlieren records we obtained revealed the salient fluid mechanical features of pulsed plasma jets.[14] They demonstrated, in particular, that the jets can be wholly subsonic or embody a supersonic core. The former was found to provide a greater depth of penetration, indicating the advantage of unrestricted opening at the exit of the plasma cavity. Moreover, physical reasons for the impressive effectiveness of the jets in entraining the surrounding atmosphere and mixing were brought out by direct experimental observations.[12] This was confirmed by MBMS measurements,[3,13] providing a rationale for the application of pulsed jets as igniters of extremely lean mixtures.

Liquid Fuel Strays

Evaporation and deformation over liquid fuel droplets at near- and super-critical conditions that are typical of low heat rejection diesel engines[1,7] was explored. Taken under particular scrutiny in this connection were conditions at a stagnation point. In order to elucidate the mechanism of the process, we introduced a number of simplifying assumptions concerning the physical properties of the substance, and expressed the energy and species conservation principles for the transient state under study in terms of transport equations for vorticity and temperature in both liquid and gas phase. These were solved simultaneously, subject to appropriate boundary conditions, to yield profiles of vorticity, temperature, and species concentrations, as well as the regression rate of the interface between the fuel and the gas stream. On this basis computations were performed for octane as a representative fuel. Its initial temperature was taken as 300°K, while the environment was assumed to be at 2300°K. Two cases were examined, the near-critical when the pressure was 0.166 MPa below the critical value of 2.526 MPa,

*This work was supported by the Office of Energy Research, Office of Basic Energy Sciences, Engineering and Geosciences Division of the U.S. Department of Energy under Contract No. DE-AC03-76SF00098, and by the National Science Foundation under Grant CPE-8115163.

and the super-critical corresponding to twice this pressure. The results demonstrated a distinct superiority of the latter in regression rate as well as in penetration depth, expressed in terms of the fuel concentration profiles.

Modeling Studies

The most significant progress in numerical techniques we developed was in the extension of the random vortex method to flow fields in enclosures via the zero Mach number model.[5,6,8,9,11] The most prominent result of these studies is the establishment of the fluid mechanical properties of flame fronts and the evaluation of their consequences in the case of flames propagating in enclosures, such as the cylinder-piston system of an engine. These are as follows: 1° advection at the local velocity of the unburnt medium, 2° self-advancement at a normal burning speed, 3° potential source due to exothermicity, 4° source of vorticity due to local baroclinic action. The first two are purely kinematic in nature, while the last two are dynamic, producing a feedback effect upon the flow field. All this applies irrespectively whether the flame is laminar or turbulent. The only difference between the two is that the normal burning speed, playing the role of an eigenvalue of the system, is, for the former, a function of the flame structure and geometry, while for the latter it is a property of the whole field. On this basis we analyzed flames propagating in containers of constant as well as variable volume, the latter simulating the piston-cylinder enclosure of an engine.[5,6] Our results demonstrated that some well-known combustion instabilities, associated with a significant distortion in flame shape, that hitherto were considered to be of acoustic origin, are basically fluid mechanical in nature.[9] Modeling of the combustion process in an engine yielded simulated pressure transducer records that were in good agreement with actual measurements.[5] Thus proper background has been laid down for the examination of the fluid mechanical consequence of some control measures, such as the substitution of a singular flame front traversing the charge, a solitary flame, by a multitude of flame kernels generated by exothermic centers that are produced by ignition jets. The igniters we developed for this purpose are described by Figs. 1 and 2. The first presents our design of a plasma jet igniter. Its prominent feature is the hollow electrode providing a duct for the introduction of proper feedstock into the cavity. The second embodies also a hollow electrode; in this case it is for the introduction of additional fuel to establish a significantly richer fuel/air mixture in the igniter cavity than that of the charge in the

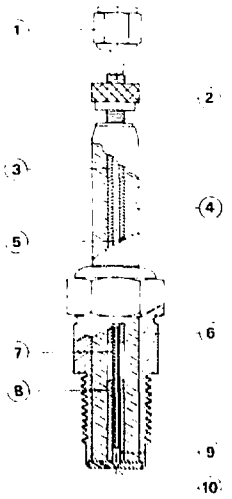

Figure 1. Plasma jet igniter; 1-tube fitting, 2-high voltage terminal, 3-steel tube, 4-insulator, 5-feedstock passage, 6-plug body, 7-nickel tube, 8-quartz tube, 9-plasma chamber, 10-discharge port. (XBL 881-302)

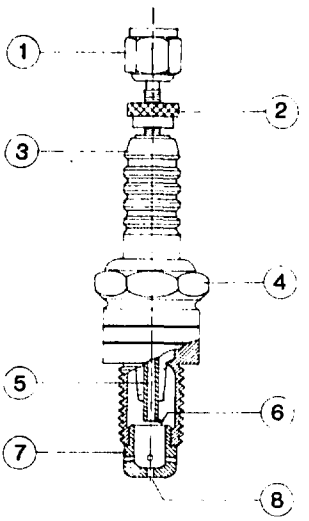

Figure 2. Flame, or hot gas, jet igniter; 1-tube fitting, 2-high voltage terminal, 3-insulator, 4-plug body, 5-nickel tube, 6-electrode, 7-injector tip, 8-discharge port. (XBL 881-303)

cylinder. The jet is thus full of hydrocarbon radicals to act as multiple ignition sources of an essentially lean working substance, providing thus the essential service for the transformation of the combustion chamber into a controllable chemical reactor, as pointed out at the outset.

PLANNED ACTIVITIES FOR FY 1988

In continuing our research on the scientific background and means for the development of controlled combustion engines, we plan to conduct a three-phase program of work.

1. Study the fundamental features of flame, or hot gas, jet ignition in a constant volume vessel using high-speed schlieren cinematography.
2. Test the performance of flame jet igniters under the influence of product recirculation, using a variable compression (C.F.R.) engine.
3. Investigate the atomization, evaporation, mixing, and inflammation of sprays produced by ultra-high pressure (~ kilobar) fuel injectors, using the shock tube apparatus we developed for this purpose.

REFERENCES

1. Lee, H.S., Fernandez-Pello, A.C., and Oppenheim, A.K. (1986), "Stagnation Point Evaporation of a Liquid Fuel at Near and Super-Critical Conditions," ASME Paper No. 86-WA/HT-15, New York, N.Y.
2. Oppenheim, A.K. (1986), "Conjectures on Controlled Combustion Engines," *Proceedings of First International Symposium on Advanced Engine Research at Wisconsin Center*, Paper 8512.
3. Cavolowsky, J.A., Breber, P.R., Oppenheim, A.K., and Lucas, D. (1987), "Pulsed Plasma Jet Igniters: Species Measurements in Nitrogen and Air," *Combustion Science and Technology*, *54*, 319-332.
4. Cavolowsky, J.A., Faris, D.W., Oppenheim, A.K., and Smy, P.R. (1987), "Formation of a Plasma Puff," SAE Paper 870609.
5. Oppenheim, A.K., and Rotman, D.A. (1987), "Fundamental Features of Ignition and Flame Propagation in Engines," ASME Paper 87-ICE-21, 8 pp.
6. Bonini, J., Xia, L.Q., Chau, E., Hom, K., Stewart, H.E., Sawyer, R.F., and Oppenheim, A.K. (1987), "Visualization of Flow and Combustion Processes in a Square Piston Engine Simulator," SAE Paper 870452, 9 pp.
7. Lee, H.-S., Fernandez-Pello, A.C., and Oppenheim, A.K. (1987), "A Model of Diffusionally Controlled Near- and Super-Critical Droplet Evaporation," *Combustion and Flame* (in press).
8. Bui, T.D., and Oppenheim, A.K. (1987), "Evaluation of Wind Effects on Model Buildings by the Random Vortex Method," *Applied Numerical Mathematics*, *3*, 1-2, 195-207.
9. Rotman, D.A., and Oppenheim, A.K. (1987), "Aerothermodynamic Properties of Stretched Flames in Enclosures," *XXIst Symposium (International) on Combustion*, The Combustion Institute, Pittsburgh, Pa. (in press).
10. Oppenheim, A.K. (1987), "Fluid Mechanical Control of Combustion," Plenary Lecture, 11th Canadian Congress of Applied Mechanics, Edmonton, Canada.
11. Rotman, D.A., Pindera, M.Z., and Oppenheim, A.K. (1987), "Fluid Mechanical Properties of Flames in Enclosures," Eleventh International Colloquium on Dynamics of Explosions and Reactive Systems, Warsaw, Poland.
12. Smy, P.R., Clements, R.M., Oppenheim, A.K., and Topham, D.R. (1987), "Structure of the Pulsed Plasma Jet," *J. Phys. D: Appl. Phys.*, *20*, 1016-1020.
13. Cavolowsky, J.A., Breber, P.R., Oppenheim, A.K., and Lucas, D. (1987), "Pulsed Plasma Jet Igniters: Species Measurements in Methane Combustion," Western States Section Meeting, The Combustion Institute, Honolulu, Hawaii.
14. Oppenheim, A.K. (1987), "Quest for Controlled Combustion Engines," Western States Section Meeting, The Combustion Institute, Honolulu, Hawaii.

Smoke Emission Measurements from Medium Scale Experiments*

R.B. Williamson, R. Dod, F.W. Mowrer†, N.J. Brown, and T. Novakov

Knowledge of the quantity and character of the smoke emitted by fires occurring in the aftermath of a post nuclear exchange is crucial for predicting its climatic impact. Sooting is controlled by a complex interplay between chemical kinetics and fluid mechanics. Relative to our understanding of elementary reactions of small species, the understanding of the chemistry of larger species (soot precursors and soot) is in a very primitive stage. It is not possible to predict the soot quantity and character from our current understanding of the chemistry. Considerable problems of scale are also associated with identifying crucial heat transfer and turbulence parameters. The performance of smoke quantification and characterization measurements over a range of scales will make positive and important contributions to this most difficult and significant problem. The measurements should be accompanied by careful documentation of combustion conditions to enable researchers ultimately to employ the results obtained in controlled laboratory situations to extrapolate to conditions believed important in various post-nuclear fire scenarios.

To help quantify the smoke which might be generated following the use of nuclear weapons, and perhaps cause "Nuclear Winter," a series of medium-scale fire experiments with representative urban fuels, such as wood, asphalt roofing and liquid petroleum, has been conducted here at LBL. These experiments have been conducted under both well ventilated and underventilated conditions, and during each experiment the mass of smoke was determined by sampling the aerosol particulate in the exhaust duct which captured all the effluent from the burning material. The rate-of-heat-release (RHR) was measured by oxygen depletion calorimetry (ODC). Sampling probes were inserted through the wall of the duct and were designed to provide isokinetic sampling of the flowing smoke and combustion products. The direct measurement of the smoke particulates and their characterization is one of the unique features of this research program.

*This work was supported by the Defense Nuclear Agency through the U.S. Department of Energy under Contract No. DE-AC03-76SF00098.

†University of Maryland, Dept. of Fire Protection Engineering, College Park, MD 20742

ACCOMPLISHMENTS DURING FY 1987

During FY 1986, 13 experiments were conducted using softwood (both solid wood and plywood) and asphalt roofing shingles. As shown in Fig. 1, the smoke emission factors measured for burning wood under well ventilated conditions were in the range of 0.1 to 0.3 percent, but under limited conditions this increased an order of magnitude to the 1 to 3 percent range. The smoke emission factors measured for asphalt under well ventilated conditions are again an order of magnitude higher, in the 14 percent range. The implications of these measurements, in the context of Nuclear Winter, center around three aspects of the measurements. First, there is a substantial effect of ventilation on the smoke production from burning wood; it is significant that the smoke emission factors measured under limited ventilation conditions were more than an order of magnitude higher than those measured in well ventilated conditions. Wood is one of the major building and furnishing materials used in the United States, and it is reasonable to assume that large quantities of wood will burn under both limited and unlimited ventilation conditions in the post nuclear environment. A second aspect of the measurements is that the "medium scale" well ventilated wood experiments produced several orders of magnitude more black carbon than had previously been reported by bench scale experiments. It is the black carbon particles which absorb sunlight and produce the "Nuclear Winter" effects. A third aspect of the measurements is that the smoke emission factors found for asphalt roofing shingles, a total of almost 14 percent with 90 percent being black carbon, may have a significant impact on urban smoke products in the nuclear environment. These results have been presented at the Second International Symposium on Carbonaceous Particles in the Atmosphere, October 5-8, 1987, Lawrence Berkeley Laboratory, University of California, Berkeley, and are described in detail in References 1 and 2.

During FY 1987, the exploration of the smoke production of liquid petroleum, which represents one of the major fuel sources in the post nuclear environment, was added to our program. Medium scale experiments with No. 2 fuel oil have been conducted under both well ventilated and limited ventilated conditions. The smoke emission factors in the 8 to 9 percent range have been measured from 400 to 800 KW for well ventilated fires. The results of the limited ventilation experiments have not been reduced at this writing, but their emission factors appeared to be greater. The average particle emissions factors for all fuels types are shown in Fig. 1.

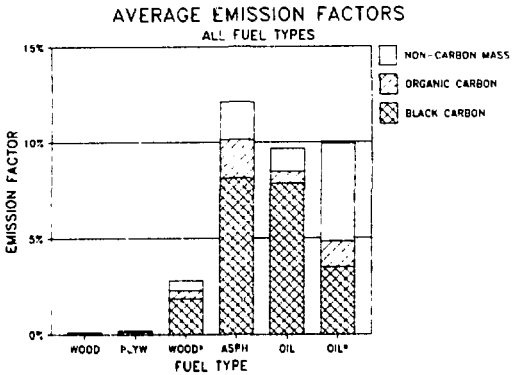

Figure 1. Histogram of the Smoke Emission Factors Measured for Various Fuels Burning under well ventilated conditions and limited ventilation conditions, marked with a *. (XBL 883-807)

PLANNED ACTIVITIES FOR FY 1988

A continuation of the medium scale experiments with increasing rates of heat release under various ventilation conditions in order to evaluate the effects of scaling. The study of scaling will be emphasized and ways of correlating the findings from these medium and large scale experiments will be explored.

REFERENCES

1. Brown, N.J., Dod, R.L., Mowrer, F.W., Novakov, T., and Williamson, R. B., "Smoke Emission Factors from Medium Scale Fires: Part 1," *Presented at the Third International Conference on Carbonaceous Particles in the Atmosphere*, October 5-8, 1987, Lawrence Berkeley Laboratory, University of California, Berkeley, CA, and submitted for publication in a special issue of *Aerosol Science and Technology*, LBL-24912.
2. Dod, R.L., Brown, N.J., Mowrer, F.W., Novakov, T., and Williamson, R.B., "Smoke Emission Factors from Medium Scale Fires: Part 2," *Presented at the Third International Conference on Carbonaceous Particles in the Atmosphere*, October 5-8, 1987, Lawrence Berkeley Laboratory, University of California, Berkeley, CA, and submitted for publication in a special issue of *Aerosol Science and Technology*, LBL-24893.

Combustion Chemistry*

N.J. Brown, R.J. Martin, and M. Longuemare

Combustion processes are governed by chemical kinetics, energy transfer, transport, and fluid mechanics, and the complex interactions among these. Understanding chemical kinetics and energy transfer offers the possibility of better understanding combustion so that it can be controlled to achieve decreased levels of pollutants and better efficiencies. In all chemical changes, the pathways for energy movement are determining factors. Competition among these pathways, including energy dissipation, determine product yields, product state distributions, and the rate at which reaction proceeds. This competition is influential in flames, explosions and shock waves. Advances of theories of reactivity have important impacts on our understanding of the chemistry affecting the emissions of pollutant species, rates of heat release during combustion, and the growth rates of undesirable combustion phenomena. The first portion of our research is concerned with understanding reactivity and energy transfer processes at the state-to-state level to determine rate-controlling factors.

The second portion of our research is concerned with understanding the combustion chemistry of nitrogenous pollutants, and is currently focussed upon nitrous oxide chemistry. Nitrous oxide is the principal source of stratospheric nitric oxide which is a major scavenger of stratospheric ozone. Nitrous oxide is also a greenhouse gas, and its residence time in the atmosphere is approximately 150 years. Its concentration in the atmosphere is increasing by 0.2% per year, and combustion is a major contributor to the budget. The factors which control N_2O

*This work was supported by the Office of Energy Research, Office of Basic Energy Sciences, Engineering and Geosciences Division of the U.S. Department of Energy under Contract No. DE-AC03-76SF00098, and by the National Science Foundation under Grant CPE-8115163.

emissions are not well understood so that it is not possible to inventory accurately anthropogenic sources other than by exhaustive source measurements. Furthermore, it is not possible to design cost-effective control strategies or to predict the efficacy of current NO_x techniques for N_2O reduction unless a more fundamental understanding of N_2O combustion chemistry is acquired.

ACCOMPLISHMENTS DURING FY 1987

Energy transfer in the coplanar, rigid rotor H_2 + H_2 system and its isotopic analogues (H_2 + HD and HD + HD) was studied with the method of classical functional sensitivity analysis. This was a collaborative research effort[1] with Herschel Rabitz and Richard Judson of Princeton University. Sensitivity Analysis is a general approach to understanding the relationship between the potential energy surface and a set of observables. The functional sensitivities measure the response of an observable to arbitrary variations of the potential at some point in configuration space.

The potential energy surface used for the H_4 system was determined by Silver and Brown[2], and this was expanded in a complete set of angular functions of the form $V_{m_1m_2}^{(R)} \cos(m_1Q_1 + m_2Q_2)$. The sensitivities for each observable were also expanded in the same set of angular functions used for the potential as shown in Fig. 1, and this enabled us to measure the importance of individual terms in the potential. Trajectory sensitivities were calculated, and then each observable sensitivity for individual trajectories was calculated using the functional chain rule. Observable sensitivities for an ensemble were determined by ensemble averaging the trajectory values, and this required approximately 1000 trajectories. Calculations are computationally very intensive. We have found that sensitivity analysis for problems of importance in molecular physics provides new and exciting information, and that this has the potential for really challenging some of the more traditional ideas about collisions.

Five major conclusions were reached as a result of this study:

(1) Small magnitude, high order terms in the potential (as measured by an expansion in a complete set of angular functions) can affect the final energy distribution in important ways.

(2) Particular terms in the potential can influence individual observables quite differently.

(3) For the isotopic combinations examined (with the possible exception (HD +HD), rotation-rotation and rotation-translation energy transfer process are approximately separable in the sense that varying a particular term in the potential will only affect energy transfer between a single pair of degrees of freedom.

(4) Rotational-translational energy transfer processes are much more sensitive to the potential than are the rotational-rotational

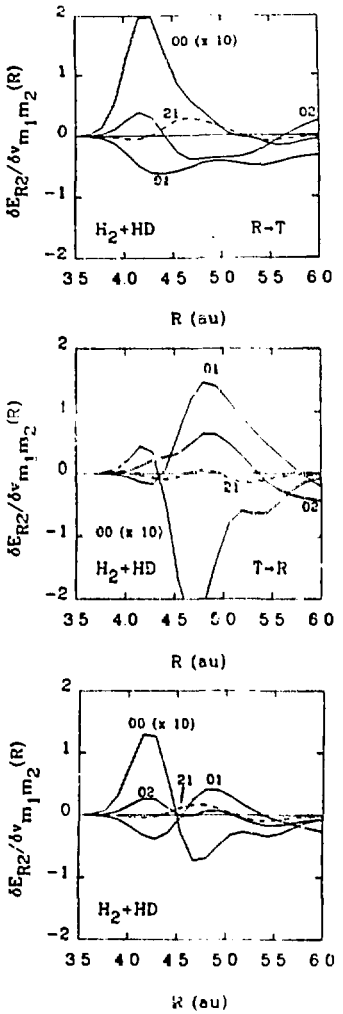

Figure 1. The largest sensitivity functions for the HD molecule for the case $H_2(j=1)$ and $HD(j=3)$. The values of all curves have been multiplied by 1000 and units are au^{-2}. The first index is the value of m1 and the second represents m2. (XBL 882-609)

ones, and this result is partially due to the use of classical mechanics. A consequence of the rotational translational dominance is that the effect of altering a term in the potential responsible for transferring energy between translation and rotation of one molecule is not very dependent on the identity of (HD or H_2) of the other molecule.

(5) The influence of the potential on the energy transfer into or out of each of a pair of identical molecules is quite sensitive to the initial rotational energy of the molecules.

Another problem that was investigated was rotational relaxation of HD. This study was performed to model the experiments of Chandler and Farrow[3] (CF) of Sandia National Laboratory. In these studies HD molecules were excited to $v = 1$ and a specific J state such that $J \leq 6$, and these collided with HD molecules in a thermal distribution at 298K. The rate coefficients required to determine the relaxation time of the excited state distribution were determined. This study was a molecular dynamics one which employed the Silver/Brown surface B. Some of the assumptions regarding the dynamics that (CF) employed in the analysis of data were investigated in our theoretical studies. Average energy transfer quantities per collision, correlation coefficients, and rate coefficients were computed. Particular attention was paid to angular momentum exchange among the three types and to whether or not there was an appreciable average change in the z component of angular momentum. Because there was more rotational-translational exchange than rotational-rotational exchange, the correlation between j_i (where $i = 1$ or 2) and orbital angular momentum was stronger than j_1 or j_2. The vibrational degrees of freedom of the two molecules were highly coupled. In our study changes of j of more than 2 angular momentum units were quite rare, and the corresponding rate coefficients for these transitions agreed satisfactorily with the values of CF.

Modeling calculations have been performed[4] to illustrate the effect of using five commonly accepted data bases of thermochemical properties on predictions of temporal species profiles. The thermochemical properties are those used for the determination of equilibrium constants employed in the calculation of reverse rate coefficients for a chemical mechanism where forward rate coefficients are specified. The modeling study was performed for hydrogen/oxygen/argon/nitrogen-compound mixtures where the nitrogen compound was either NO or NH_3. The mixtures reacted isothermally at 1600 K and isobarically at 1 atmosphere, and a single kinetic mechanism for which forward rate coefficients were specified was used throughout. Mixtures of equivalence ratios of 0.625, 1.0 and 1.6 were considered. Modifications in sources of thermodynamic data have been substantial since 1971 for some species. Among the data bases, thermochemical properties varied greatly for the species NH, NH_2, NNH, and HO_2, and those for other species important in the mechanism had variations of less than 10 percent. The single most important result of our study is that the thermochemical property variations for NH, NH_2, NNH and HO_2 among the data bases have substantial effects upon the temporal species profiles for nitrogenous species. This is most pronounced for rich combustion, and varies directly with equivalence ratio. Use of different data bases had little effect on the H/O species profiles. Radical species profiles (with the exception of HO_2) tend to be influenced strongly by their own thermochemical properties. Computed profiles also were shown to be independent of algorithm (HCT or CHEMKIN) and thermodynamic property fitting procedure between 1000 and 2000 K.

Nitrous oxide production and destruction were investigated in laminar, one dimensional atmospheric pressure flames[5]. The experimental variables were bulk flow rate, equivalence ratio, nitrogen compound type, nitrogen concentration, and fuel type. Radial and axial temperature and composition profiles were measured. Nitrous oxide is formed in lean CH_4/air and H_2/air flames doped with N_2, NO, N_2O, and NH_3, but it does not survive into the post flame zone. Nitrous oxide concentration was found to depend inversely upon final flame temperature and equivalence ratio and directly upon nitrogen compound concentration. In decreasing order of observance of early N_2O, the four dopants can be ranked: N_2O, NH_3, NO, and N_2. Nitrous oxide profiles were similar in both CH_4 and H_2 flames. Radial profile measurements showed increased amounts of N_2O existing near the burner edge. Modelling calculations were also performed for the H_2 flames with the four nitrogen dopants. Comparison between calculated NO and N_2O profiles and those measured in the flame showed that our understanding of nitrogen combustion chemistry is still deficient.

PLANNED ACTIVITIES FOR FY 1988

Research in both of these areas will continue.

REFERENCES

1. Judson, R.S., Rabitz, H., and Brown, N.J. (1988), "A Classical Functional Sensitivity Analysis of Coplanar Inelastic Scattering for $H_2 + H_2$ and its Isotopic Analogues," to be submitted to *J. Chem. Phys.*
2. Silver, D.M., and Brown, N.J. (1980), "Valence Bond Model Potential Energy Surface for H_4," *J. Chem. Phys. 72*, 3859.
3. Chandler, D.W., and Farrow, R.L. (1986), "Measurement of Rotational Energy Transfer Rates for HD (v=1) in collision with Thermal HD," *J. Chem. Phys. 85*, 1733.
4. Martin, R.J., and Brown, N.J. (1988), "The Importance of Thermodynamics to the Modeling of Nitrogen Combustion Chemistry," submitted to the Twenty-Second International Symposium on Combustion.
5. Martin, R.J., and N.J. Brown (1988), "Formation and Destruction of Nitrous Oxide in Lean Premixed Combustion," presented at the Joint Western States and Japanese Sections Meeting, The Combustion Institute, Honolulu, Hawaii.

Combustion Fluid Mechanics*

R.K. Cheng, I.G. Shepherd, and L. Talbot

Although it is well known that fluid mechanical turbulence increases the overall combustion reaction rate, the exact relationship between turbulence intensity and mean burning rate remains a major unresolved issue in fundamental turbulent combustion research. The overall goal of this program is to gain a better physical understanding of the controlling turbulence-combustion interaction processes through detailed study of the complex turbulent combustion flowfields in simplified laboratory scale burners. By the use of laser diagnostic techniques which measure scalar and velocity fluctuations and cross-correlations, the detailed statistical data are obtained for comparison with predictions of theoretical models and for determining burning rates.

ACCOMPLISHMENTS DURING FY 1987

In FY 1987 we have developed a new experimental procedure and method of analysis to deduce the turbulent burning rate $\bar{w}$[1]. This study is motivated by the fact that to date, the most convenient means to express the increase in burning rate is by the use of the turbulent burning speed, S_T. The large uncertainties associated with determining S_T using the conventional flame orientation method have been reported in the literature. In many cases the results have been shown to be rather meaningless[2]. Consequently, reliable S_T data has only been obtained in configurations specially designed to reduce the uncertainties but not in practical burners which have complex flame geometries. Therefore, an alternate means to determine S_T which is independent of flame geometry is highly desirable.

Our analysis is based on capitalizing recent theoretical works of Bray and co-investigators. Central to their theory is a model of the reaction rate which is expressed in terms of the the mean flame crossing frequencies, ν. The most significant feature of the crossing frequency concept is that ν can be measured directly in experiments using simple laser techniques. Their latest model (Bray, Champion and Libby (BCL)[3], indicates a convenient means to investigate the functional relation between S_T and $\bar{w}$. This important aspect of premixed turbulent flame propagation has remained largely unexplored by experiment. The significance for theoretical developments is that the relationship between $\bar{w}$ and S_T could be used in validating the model and obtaining new closure techniques for predicting the burning rate.

The model treats the turbulent flame region as consisting of a thin wrinkled fluctuating flame interface which separates the the unburned reactants from the burned products. Under the fast chemistry assumption, this scalar quantities can be represented by a single progress variable, c. The second and third order turbulent transport terms can then be expressed in terms of c and the conditioned velocities in the reactants and products zones U_r,U_p. The reaction rate $\bar{w}$ is expressed by a simple equation $\bar{w}(x) = w_f(x)\nu(x)$ where ν is the number of flame crossings per unit time and w_f is the mean rate of creation of products by each crossing. By further assuming that the flame sheet consists of laminar

*This work was supported by the Director, Office of Energy Research, Office of Basic Energy Sciences, Chemical Sciences Division of the U.S. Department of Energy under Contract No. DE-AC03-76SF00098.

flamelets, BCL [3] models w_f as $w_f = \rho_r S_L / U_n$ such that

$$\overline{w} = \frac{\rho_r S_L \nu(x)}{U_n(x)}$$

where S_L is the laminar burning speed of the flamelet and U_n is the mean convection speed of the flamelet with respect to the laboratory frame.

The most significant feature of this model is its simple relationship to the turbulent burning speed. For a one dimensional flame, it can be demonstrated that the integration of the reaction rate from $x = 0 \rightarrow \infty$ determines the turbulent burning rate. By analogy to the laminar burning rate $\rho_r S_L$, the turbulent burning rate is $\rho_r S_T$. Therefore,

$$\int_0^\infty \overline{w}\, dx = \rho_r S_L \overline{W} = \rho_r S_T$$

where

$$\overline{W} \equiv \int_0^\infty \frac{\nu(x)}{U_n(x)}\, dx$$

$\overline{W}$ is the ratio between the turbulent burning rate and the laminar burning rate and is identical to the turbulent/laminar burning speed ratio S_T/S_L.

To verify Equation (1), experimental measurements of $\overline{w}$ in the two configurations were carried-out. The configurations are 1) rod-stabilized oblique v-flames and 2) large Bunsen conical flames. The flame crossing frequencies ν are measured by monitoring the Mie scattering from a silicone aerosol introduced into the reactant stream. The technique is based on the principle that the oil droplets evaporate and burn at the thin flame front. Since our analysis involves integrating the experimental data obtained through the flame brush, the choice of traverse trajectories is significant. In the past, data have been obtained along fixed vertical or transverse axes in laboratory coordinates. This was due mainly to limitations in the traversing mechanism for the diagnostic probe. A more logical choice is to measure along the mean flowlines i.e. the Lagrangian lines.

Since our setup consists of a computer controlled data acquisition system interfaced with a three dimensional traverse laser table and a two component laser Doppler anemometry (LDA) system, it is possible to trace automatically a flowline as specified by the local two dimensional unconditioned velocity vector. Figure 1 shows examples of the mean flowlines measured in the v-flame and in the conical flame. From a starting point x_0 and y_0 within the reactants, the system determines the next measurement position by measuring and computing the mean velocity components $\overline{U}$ and $\overline{V}$, then moves the LDA probe by a fixed increment in the direction of the velocity vector.

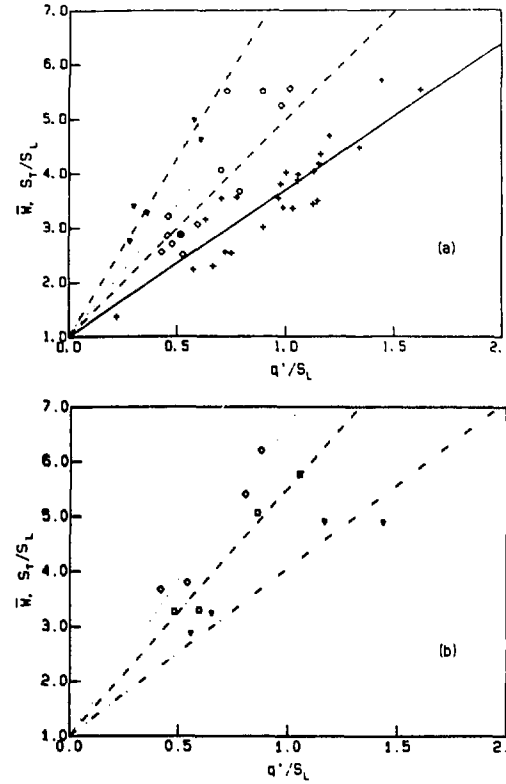

Figure 1. Typical 2D mean Lagrangian flowlines used for flame traverse and $\overline{c}$ = 0.1 and 0.9 contours for v-flame and conical flame. (XBL 8712-5389)

There are several laser diagnostics techniques suitable for measuring the convection speed of the flame fronts, U_n. However, these techniques are not very convenient for collecting large amount of data for statistical analysis. Since previous studies have shown that U_n in both of the configurations are very close to the mean flow velocity, for our analysis we have used the conditioned velocity in the reactants.

Measurements were made in five v-flames and four conical flames using methane/air mixture with various equivalence ratios and incident turbulent intensities. For each flame, two flowlines initially at

y_0 = 10 and 20 mm from the centerline were traced through the flame brush. In addition, traverses along the centerlines of the conical flame were also made. The values of $\overline{W}$ were determined by integrating ν/U_r along these flowlines. Since $\overline{W} = S_T/S_L$, they can be compared directly on the conventional S_T/S_L versus q'/S_L plane where q' is the turbulent kinetic energy of the incident flow. Shown in Fig. 2(a) is the correlation of $\overline{W}$ in the v-flames with q'. Also shown are the ratios S_T/S_L in CH_4 / air stagnation point stabilized flames under similar flow conditions. The results determined previously for ethylene/air v-flames using the flame orientation method are also plotted for comparison. The various sets of results are fitted linearly by a least mean square. It is apparent that our $\overline{W}$ results are in good agreement with those of the stagnation point flames. They are also consistent with those deduced by the flame orientation method. However, the present analysis is a significant improvement since the uncertainty based on integrations is substantially reduced.

The result obtained in the conical flames are shown in Fig. 2(b). In contrast to the v-flame results, the conical flame results show a consistent trend of increasing $\overline{W}$ towards the flame tip region. This is better illustrated by fitting separately the results obtained on the centerline, at y_0 = 10.0 and 20.0 mm. The profiles with y_0 = 20.0 mm are within the oblique flame zone and closest to the burner rim. The most significant aspect of the conical flame results is that prior to this study, the burning speed along the centerline has not been reported because as mentioned earlier the flame orientation method implies that the turbulent burning speed is equal to the approach flow velocity. By using the flame crossing frequency method, we have demonstrated that the turbulent burning speed can be determined with confidence in more complex flame geometries.

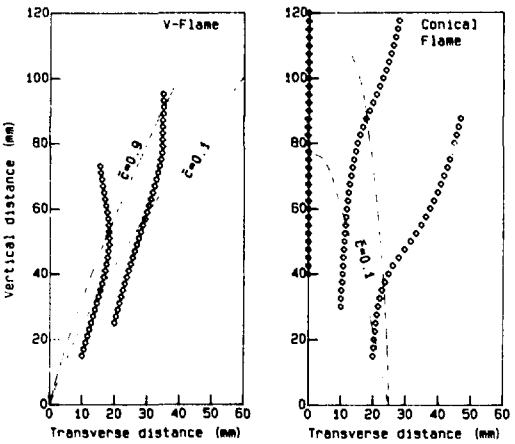

Figure 2. Correlation of the turbulent burning rate $\bar{w}$ with incident turbulence intensities (a) comparison of the results in v-flames (broken lines) and stagnation flow stabilized flames (solid line). (b) Comparison of $\bar{w}$ obtained in the conical flames along flowlines originating at y_0 = 20, 10, and centerline. (XBL 8712-5390)

In addition to our experimental works, progress has also been made in our numerical study of premixed turbulent flames using the vortex dynamic technique. As reported in FY 1986, the numerical work complements the experimental studies and assists in determining the controlling process for turbulent productions due to combustion. In FY 1987, we have explored the means to improve the algorithm for describing the movements of the flame interface. The technique used in the previous study assumes that the flame fronts advance normal to the local flame tangent at the laminar burning speed. This technique cannot consider the effects of flame curvature on local burning speed and does not permit the flame interface to form into flame cusps. A new flame movement algorithm develop by Prof. J. Sethian for vortex dynamic simulations of premixed turbulent flames is capable of overcoming these limitations. This algorithm is being incorporated into our numerical program for the v-flames.

PLANNED ACTIVITIES FOR FY 1988

The method of determining the turbulent burning speed for premixed turbulent flames will be used to conduct a parametric study to correlate S_T with turbulence of various intensities and length scales. The experiments will be carried-out in conical flames, stagnation point stabilized flames, and in open and partially enclosed v-flames. One of the most interesting implication of the relationship between the reaction rate and turbulent burning speed is that the turbulent/laminar burning speed ratio is also directly proportional to the increase in flame area due to turbulence. In FY 1988 we plan to conduct a tomographic study of the flame front dynamics and flame geometries using a video camera system interfaced with the image analysis system. The shape and size of the flame wrinkles and the flame area in two-dimension can be determined and compared with theoretical predictions.

The vortex dynamics simulation of the v-flame will be extended to include the new algorithm which

considers the variation of the flame speed due to curvature. The evolution of the shape of the flame interface predicted by this model will be compared with those shown by tomography. Also deduced from the numerical results are the conditioned velocity statistics which can be compared with previously obtained experimental data.

The study of non-premixed (diffusion) turbulent flame will be initiated. Our approach is to investigate non-premixed turbulent flames at moderate to low Reynolds numbers. All of the diagnostic techniques and associated data reduction methods can be used for this study. A turbulent jet flame burner with adjustable co-flowing air will be constructed.

REFERENCES

1. Cheng, R. K., and Shepherd I. G. (1988), "Reaction Rates in Premixed Turbulent Flames and their Relevance to the Turbulent Burning Speed", to appear *22th International Symposium on Combustion.*
2. Cheng, R. K., and Ng, T. T. (1984), "On Defining the Turbulent Burning Velocities in Premixed V-shaped Turbulent Flames", *Combustion and Flame*, 57, p. 155.
3. Bray, K.N.C., Champion, M., and Libby, P.A. (1988), "Reaction Rates in Premixed Turbulent Flames," *22th Internation Symposium on Combustion.*

Photochemical Conversion of Solar Energy by Microbial Systems*

L. Packer, R.J. Mehlhorn, I.V. Fry, J.J. Maguire, S. Spath, K. Tsujimoto†, W. Nitchmann, E. Hrabeta-Robinson, M. Huflejt, J. Hrabeta, M. Semadini and C. Reveron‡

The Membrane Bioenergetics group is currently investigating biological oxidations and bioenergetics in three areas: i) cyanobacteria, ii) bacteriorhodopsin (bR), and iii) bacterial succinate dehydrogenase (SDH). An overview of our most recent and novel results is presented, with the pertinent references to our publications.

ACCOMPLISHMENTS DURING FY 1987

Cyanobacteria

Cyanobacteria are a versatile species whose biochemistry readily adapts to changes in environmental conditions. Stress conditions (salinity) were used as a probe to investigate these adaptive processes on both functional and structural-compositional levels. Magnetic resonance spectroscopy (NMR and EPR) proved to be useful non-invasive tools for monitoring adaptive changes in whole cells of *Synechococcus* 6311 after a transition from low (0.01 M) to high NaCl (0.5M).

Structural-compositional Studies

During the past year we have clarified the temporal sequence of responses accompanying salt stress and adaptation. Using ^{23}Na- and ^{31}P-NMR analysis it was shown that the rapid penetration of Na^+ resulted in the disruption of ATP synthesis. However, during adaptation, the pattern of ^{31}P metabolites was similar to control cells, except that they produced more (and more intense) peaks in the monoester sugar phosphate region. The gross effects of stress were manifest as decreases in growth rate, photosynthesis, increases in respiration, sodium proton exchange activity and glycogen content. Examination of cells during various stages of the stress and adaptation process using flow cytometry, thin section and freeze fracture electron microscopy, showed that one minute after salt shock, virtually all the intracellular granules disappeared, the density of the cytoplasm decreased and the appearance of DNA material was changed. Four hours after salt exposure there was a reappearance of glycogen (preferentially between the cytoplasmic membrane and the thalykoid membrane) and other granules. At this time the photosynthetic oxygen evolution rate began to recover and respiratory activity was already substantially elevated. A decrease in the total number of membrane particles was observed at 4 hours with a shift from small to large particle size. After 24 hours the particles increased in total number and the large sized particles predominated. This pattern was not observed in the cytoplasmic membrane of control cells and it suggests synthesis of new membrane proteins in agreement with the known increases in cytochrome oxidase and sodium proton exchange activity[1-3].

Functional Studies

Concomitant with the structural-compositional changes, respiratory adaptations were also evident. *De novo* synthesis and levels of the terminal electron acceptor, cytochrome *c* oxidase, were investigated using purified cytoplasmic membranes which exhibited low temperature EPR spectra in the g = 2.08 region. This characteristic copper signal arose from a center in an environment identical to the aa_3-type cytochrome *c* oxidases reported in mammalian, yeast and bacterial systems. Membrane purification procedures demonstrated that the oxidase was present in the cytoplasmic membrane at ten times the level present in the thylakoid membrane. The copper was demonstrated to be fully redox active by its reducibility with physiological electron donors[4,5].

Applications of Cyanobacterial Productivity

The feasibility of using photosynthetic microalgae as a component in a Controlled Ecological Life Support Systems (CELSS), with particular emphasis

*This research was supported by the Office of Basic Energy Sciences of the U.S. Department of Energy under contracts DE-AC03-76SF00098 and DE-FG03-87ER13736 and NASA Interagency agreement A-14563c.

†Visiting associate professor, on leave from the University of Electro-communication, Chofu, Tokyo.

‡LBL/JSU/AGMEF Summer Faculty Programs.

on the manipulation of biomass components was addressed. Using factors which retard growth but not photosynthesis, the partitioning of photosynthate may be directed towards carbohydrate and away from protein synthesis. Cold shock of dense cultures increased the glycogen content from 1% to 35% dry weight, and presents a technique to change the protein/carbohydrate ratio to a nutritionally acceptable level[6].

Antioxidative Effects of Organic Ge

The effects of an organic germanium sesquioxide (Ge-132) complex on the biochemistry of the cell was determined. The experimental approach was to assess concentration dependent toxic effects, by growth curve analysis, to monitor the bioenergetic impact of Ge-132 on photosynthesis and respiration, and to determine the assimilation and cellular distribution of germanium.

Bacteriorhodopsin

Bacteriorhodopsin (bR) is a protein in the purple membrane regions of the cytoplasmic membrane of *Halobacterium halobium* which translocates protons upon light absorption, and is one of the simplest known biological pumps. To elucidate the molecular mechanism, the role of amino-acid residues in the photocycle, and how this relates to cation binding was investigated using chemical modification of carboxyl and tyrosine residues. The proton pumping activity was affected only in the case of iodinated tyrosine samples. Modification of carboxyl residues influenced the time course of the photocycle but did not change the number of pumped protons per photocycle and the R-values evaluated. The effects of cation binding to chemically modified carboxyl groups were studied. Visible and EPR spectroscopy showed that two cations bind on the surface and at least one site is located in the protein interior. The fractional conversion of the blue to purple species by cation titration, heat treatments (cation release) and Mn binding showed that internal cross-linking or tempamine labeling disrupts cooperativity and weakens the cation binding site. Thus, internal and external carboxyl residues, and structural mobility within bR are essential to formation of the cation binding site. White membranes from the JW-5 strains reconstituted with all-trans retinal (WMrec) were also found to form the blue species. In this case, titration studies showed that up to 100 divalent cations bind to reform purple species. WMrec shows less cooperative association than in native bR, however, heat treatment studies suggest a greater stabilizing effect of cations on the structure of the WMrec than bR. Hence, negatively charged lipids in WMrec regulate cation binding[7-11].

Succinate Dehydrogenase (SDH)

An understanding of the mechanism, structure and assembly of complex metalloenzymes is important in understanding the complex interactions that exist between the transport of electrons through protein complexes and the relationship between protein electron transport and biological energy transduction. Little is known about the structure and the assembly-functional integrity of complex membrane proteins. In order to address this question mutants of *Bacillus subtilis* with specific lesions in the succinate dehydrogenase redox complex were analyzed using gene mapping, low temperature EPR and molecular weight analysis of native and truncated fragments of the protein subunits. The following new information about the assembly of one of the covalently bound iron sulfur clusters, cluster S-2, was determined. It can be assembled in the cytoplasm in the absence of the native binding protein (cytochrome *b*), and it can be assembled in truncated fragments of the Ip polypeptide which contain clusters S-1 and S-2. Based on the inferred amino acid sequence from the DNA sequence there exist three conserved clusters of cysteinyl residues which are the likely binding sites for the iron-sulfur clusters. Indirect evidence indicates that the first two of these conserved clusters, from the N terminal end, are the binding sites for iron-sulfur clusters S-1 and S - 2[12].

PLANNED ACTIVITIES FOR FY 1988

Cyanobacteria and Halobacteria

In the coming year, a new NMR facility in the Life Sciences Annex will be dedicated to biological research. We forsee this as a powerful tool in our research program for the non-invasive analysis of bioenergetics and structural composition in whole cell systems. In addition, the development of new fluorescent techniques to measure intracellular pH in cyanobacteria and halobacteria will augment our non-invasive magnetic resonance investigation.

Cyanobacteria

Cytoplasmic and thylakoid membranes will be separated by established procedures, and the primary adaptive response to stress, in terms of structure and functional changes will be analyzed. Functional studies, such as ion flux, electron transport and enzyme

function, will be determined by EPR (low temperature and spin probe methods). Structural information will be derived using spin-spin interactions of membrane bound ESR probes, surface charge densities using Mn binding characteristics and by fatty acid and lipid analysis.

Succinate Dehydrogenase

Experiments will focus on succinate-quinone reductase from bacteria and mitochondria. Mechanisms and sequence of assembly of membrane metallo-enzymes are poorly understood. By using enzyme which is defective genetically, further definition of the sequence of the assembly of this enzyme will be described by measurement of an iron sulfur cluster in an enzyme fragment. Secondly, genetically defective enzyme, which is inactive enzymatically, but has defined prosthetic groups attached, will be hybridized with selected native and mutated enzyme fragments. Expression of enzymatic activity will be used to assess the essential enzyme constituents required for assembly of an intact enzyme.

The enzyme complex consists of six distinct electron/hydrogen carriers, and the pathways of electron flow will be studied using photo-reduction, laser flash photolysis and EPR to define electron flow sequences, using native and mutated enzyme. Succinate-quinone reductase from the bacterial membrane will be purified as the first step toward determining the crystal structure of this enzyme complex.

REFERENCES

1. Packer, L., Spath, S., Martin, J., Roby, C., and Bligny, R. (1987). "^{23}Na and ^{31}P NMR Studies of the Effects of Salt Stress on the Fresh Water Cyanobacterium Synechococcus 6311," *Archives of Biochem. Biophys., 256(1)*:354-361.
2. Packer, L., Spath, S., Martin, J.B., Roby, C., and Bligny, R. (1987). "^{23}Na and ^{31}P-NMR Studies of Salt (NACL) Stressed Fresh Water Cyanobacteria," *Proceedings of the 4th International Conference on Water and Ions in Biological Systems*, pp. 24-28, Bucharest, Romania (in press).
3. Lefort-tran, M., Pouphile, M., Spath, S., and Packer, L. (1988). "Cytoplasmic Membrane Changes During Adaptation of the Fresh Water Cyanobacterium *Synechococcus* 6311 to Salinity," Plant Physiology (in press).
4. Peschek, G., Trnka, M., Molitor, V., Fry, I., and Packer, L. (1988). "ESR Spectrometric and Immunochemicals Characterization of the Cytochrome Oxidase in Isolated and Purified Plasma Membranes from the Cynanobacterim *Anacystis nidulans*," submitted for publication.
5. Fry, I.V., and Peschek, G.A. "EPR detectable Cu^{2+} in *Synechococcus* 6301 and 6311: the aa_3 type cytochrome c oxidase of the cytoplasmic membrane," *Methods in Enzymology* (in press).
6. Fry, I.V., Hrabeta, J., D'Souza, J., and Packer, L. (1987). "Application of photosynthetic N_2-fixing cyanobacteria to the CELSS program," *Adv. Space Research, 7*: 39-46.
7. Packer, L., Hrabeta-Robinson, E., Stefka-Hristova, G., Toth-Boconadi, R., and Keszthelyi, L. (1987). "Proton Translocation by Chemically Modified Bacteriorhodopsin," *Biochem. International, Vol. 14, No. 6*, pp. 977-985.
8. Packer, L. (1986). "Bacteriorhodopsin: Molecular Biology of the Light Activated Proton and Divalent Cation Receptor in the Membranes of the Halobacteria, in: Membrane Receptors, Energetics, and Dynamics," Edited by K. Wirtz, Plenum Publishing Co.
9. Packer, L., and Hrabeta-Robinson, E. (1988). "Surface Charge Modification of Bacteriorhodopsin," *The Laura Eisenstein Memorial Symposium* (in press).
10. Hrabeta-Robinson, E., Semadeni, M., and Packer, L. (1988). "Cation Binding by Bacteriorhodopsin in Purple and White Membranes," submitted for publication.
11. Packer, L., Hrabeta, E., Robinson, A.E., Abdulaev, N.G., Kiselev, A.V., Taneva, S.G., Toth-boconadi, R., and Keszthelyi, L. (1987). "Effect of cross linkers on the Bacteriorhodopsin Photocyle" *Biochem. and Biophys. Res. Comm. 145(3)*: 1164-1170.
12. Cammack, R., Maguire, J.J., and Ackrell, B.A.C. (1988). "Mechanisms of electron transfer in succinate dehydrogenase and fumarate reductase; possible functions for iron-sulphur centre 2 and cytochrome *b*," LBL-25071, submitted for publication.
13. Belkin, S., Mehlhorn, R.J., and Packer, L. (1987). "Proton gradients in intact cyanobacteria," *Plant Physiol. 84*: 25-30.

Development and Application of New Assays of Oxidative Damage*

R.J. Mehlhorn, K. Moore, B. Stone, J. Fuchs and L. Packer

This project is concerned with the development of sensitive and specific assays for oxidative damage in biological systems. These assays are being used to measure free radicals and other oxidants that arise during normal mammalian metabolism and under pathological conditions.

ACCOMPLISHMENTS DURING FY 1987

Electron Spin Resonance (ESR) Traps for Free Radicals

Free radicals are highly reactive molecules that are produced when molecular bonds are broken. They are responsible for the lethal effects of ionizing radiation. More recently, free radicals associated with normal or abnormal metabolism have been implicated in disease and, possibly, aging, and this has led to great interest in understanding and ameliorating the effects of these adventitious free radicals.[1] Because of their high chemical reactivity, free radicals do not accumulate sufficiently to be observable. This problem has recently been solved by the introduction of "spin traps," molecules that stabilize free radicals so that they can be observed and identified.[2] In collaboration with K. Hideg of Pecs, Hungary, we have synthesized a free radical trap that offers considerably greater stability than previously available spin traps. The new compound is shown in a reaction with the very destructive hydroxyl radical as shown in Figure 1.

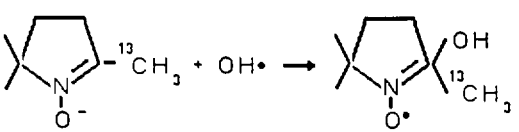

Figure 1. Reaction of the carbon-13 spin trap with the hydroxyl radical. (XBL 881-146)

*This research was supported by NIH (AG-04818) and LBL Director's funds for innovative research through the U.S. Department of Energy under contract DE-AC03-76SF00098 and by the National Foundation for Cancer Research.

In this reaction the hydroxyl radical adds to the unsaturated carbon position in the ring, forming a nitroxide free radical, which is considerably more stable than the initial hydroxyl radical and can be observed in an ESR instrument. The introduction of a carbon-13 methyl group into the spin trap ensures that a free radical adduct will not be susceptible to further oxidation, resulting in the enhanced stability of this trap compared to previously available reagents. Moreover, the nuclear spin on the carbon-13 interacts with the unpaired electron in the free radical to yield distinctive spectra for different radical adducts that serve to identify the chemical structures of free radicals that have been trapped. This is illustrated in Figure 2, where reaction products of the new spin trap with three different, biologically important, free radical species are shown.

Detection of Free Radicals and Transition Metal Ions with Hydroxylamines Derived from Nitroxides

Nitroxide "stable" free radicals, although highly persistent in biological environments, are susceptible to reduction by one-electron donors, resulting in hydroxylamines. These hydroxylamines are

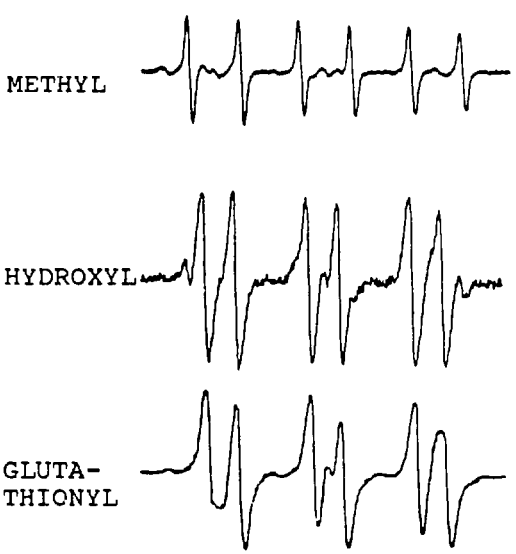

Figure 2. ESR spectra of three free radical adducts with the carbon-13 spin trap, demonstrating that biologically important oxidants can be identified with this tool. (XBL 881-145)

readily re-oxidized by a variety of free radicals and transition metal ions. We have shown that both the reduction and oxidation can be used to study free radical processes. Recently, we showed that comparative studies of reduction rates of nitroxides of different structures can be used to discriminate between major reducing agents in biological tissues.[3] We observed that ascorbic acid, which has generally been considered to be the most important reductant for nitroxides in animal tissues is a potent reductant for the piperidine nitroxide Tempol, but has little effect on pyrroline nitroxides. On the other hand, reduced flavin mononucleotide (FMN), which is a more powerful reducing agent reduces both piperidine and pyrroline nitroxides at comparable rates. From this reduction study we concluded that an analysis of reduction rates of different nitroxides can be used to analyze biological tissues for their content of ascorbate and other reductants.

Hydroxylamines derived from nitroxides by chemical reduction have proven useful for the detection of one-electron oxidants, including free radicals. In particular, we have observed that the hydroxylamine derived by a one-electron reduction from 2,2,6,6-tetramethyl-piperi-dinoxyl-4-ol (Tempol), designated as TOLH, is oxidized by phenoxyl radicals. We have exploited this fact to develop TOLH as a tool to detect oxyl radicals. In addition, we have found that TOLH oxidation, in the presence of the enzyme horseradish peroxidase and micromolar concentrations of phenol, can be used for the quantitative determination of hydrogen peroxide in tissue homogenates and cell fractions.

We have also observed that the oxidation of TOLH is mediated by traces of copper and iron ions, an effect that is strongly modulated by chelating agents. This observation has led us to develop an assay for the presence of free transition metal ions in biological systems. The assay consists of measuring the rate of TOLH oxidation in the presence and absence of membrane-permeable chelating agents that sequester the ions. The possibility that transition metal ions might be free in cells has been of great interest because of their potential as sources of free radicals in the presence of hydrogen peroxide. Among promising new research opportunities, this tool will enable us to determine whether there are pathological conditions or environmental stresses that cause such ions to be released in cells and whether there are drugs that can prevent their harmful effects.

Free Radical Traps that Produce Volatile Products

While free radical studies *in vitro*, such as those that can be obtained with spin trapping, are very useful for inferring reaction mechanisms, it is generally acknowledged that the *in vivo* implications of such studies, particularly for higher animals, are clouded by the complexity and diversity of possible responses of multicellular organisms to oxidative stress. Therefore, the development of oxidative damage indicators that report on the net effect of some stress on higher animals has been of considerable interest. Among the most encouraging recent developments are highly sophisticated analytical tools for detecting oxidation products in urine and in breath.[4] We have been interested in the potential of breath analysis, both as a research tool and as clinical diagnostic aid. A review of the current state-of-the-art has led us to identify a promising breath analysis research tool that offers high sensitivity and specificity. In collaboration with H. Rapoport of LBL, we are developing a novel radiolabeled free radical trap, tritiated 4-keto thiometyl butyric acid (KTBA), which will fragment into several products after reaction, liberating a radiolabeled gas that can be collected in the expired breath of an animal.

Free Radicals and Antioxidants in Skin

We investigated the free radical-reducing activity in skin, using nitroxide radicals as model compounds for endogenous radicals. The skin was derived from hairless mice. Nitroxide reduction rates vary considerably depending on the structure of the nitroxide. Five-membered ring pyrroline nitroxides exhibit consistently better stability than six-membered ring piperidine nitroxides. The substantially higher reduction rate observed for six-membered rings in mouse skin suggested a major role for ascorbic acid as a free radical reducing agent. This inference was confirmed by treating skin homogenates with ascorbate oxidase, which greatly inhibited reduction of the nitroxides. However, an appreciable reduction rate was observed for even the most stable five-membered rings, indicating that non-ascorbate reduction is an important alternative pathway for reducing nitroxides in skin. Among these non-ascorbate reduction pathways, thiols appear to play a major role, since treatment of skin homogenates with the thiol reagent N-ethyl maleimide substantially inhibited reduction.

PLANNED ACTIVITIES FOR FY 1988

The new traps being synthesized will be tested in both model systems, including transition metal catalyzed hydroxyl radical generators, peroxiding lipids in model membranes, cellular and subcellular systems, e.g., erythrocytes and mitochondria, and animals (rats). We will establish the sensitivities and specificities of the assays and seek to quantitate "background levels" of free radicals that occur in the absence of stress. This will set the stage for analyzing oxidative damage associated with stress, including the effects of gaseous substances like ozone and radon, water-borne hazards like heavy metals and organic pollutants, and free radical sources of clinical interest, e.g., ionizing radiation, hyperbaric oxygen and quinone anticancer drugs. These studies will extend into future years.

REFERENCES

1. Mehlhorn, R.J., and Cole, G. (1985), "The Free Radical Theory of Aging: A Critical Review." *Adv. Free Radical Biology and Medicine, 1:* 165-223.
2. Janzen, E.G. (1980), "A Critical Review of Spin Trapping in Biological Systems, In: *Free Radicals in Biology, Vol. IV*, W. A. Pryor, ed., pp. 116-154, Academic Press, New York.
3. Belkin, S., Mehlhorn, R.J., Hideg, K., Hankovsky, O., and Packer, L. (1987), "Reduction and Destruction Rates of Nitroxides," *Arch. Biochem. Biophys., 256:* 232-243.
4. Lawrence, G.D., and Cohen, G. (1985), "*In vivo* Production of Ethylene from 2-Keto-4-Methylthiobutyrate in Mice," *Biochem. Pharmacol. 34:* 3231-3236.

Impacts of Large Extraterrestrial Bodies and Mass Extinctions*

F. Asaro, H.V. Michel, W. Alvarez and L.W. Alvarez

Two enormous Ir anomalies are found in Archaean spherule-enriched layers in South Africa. Chemical measurements suggest an impact source is currently the most viable explanation.

New measurements have shown there are distinct small Ir peaks directly above the huge K-T Ir spike which disappear when ratios to clay abundances are taken. The resulting curve is continuous (as well as nearly exponential), and the smooth nature precludes episodic volcanism as a cause.

In studies of the limestone sediments near Gubbio, Italy over a 5 million-year span, only the region within about 1-1/2 meters of the K-T boundary shows any Ir anomalies above the background of ~ 13 ppt.

ACCOMPLISHMENTS DURING FY 1987

In collaboration with Donald R. Lowe and Gary R. Byerly from Louisiana State University (LSU), we have made a detailed chemical study on 104 Early Archaean (~ 3.5 billion years old) rock samples from South Africa and Western Australia. Two layers of spherule-bearing rocks in South Africa were found to have enormous enrichments of Ir. The lower layer, near the base of the Fig Tree (geological) Group of the Barberton Greenstone Belt, had up to 76 parts-per-billion of iridium (Ir) per gram of rock (ppt) and the upper layer, which varied from 50 to 200 meters higher than the lower, had up to 162 ppb. The Ir content varied considerably in different sections and was inversely correlated with reworking by current activity.

Studies of ultramafic rocks in the Greenstone Belt showed much lower levels of Ir than the maxima found in the spherule beds and argue against a volcanic origin. The measurement of 28 other elements by high precision, neutron activation analysis techniques at LBL and other elements by x-ray fluorescence at LSU suggest the impact of a large asteroid or comet is the most viable explanation for the spherules. More definitive measurements are needed, particularly of the abundances of other platinum group elements, to critically test this hypothesis.

A spherule bed found in the Warrawoona Group of the Eastern Pilbara Block in Western Australia contained up to 4.5 ppb Ir. These spherules may also have been caused by impact but the evidence is not as strong as for the South Africa beds.

A geochemical study has been made of nearly 60 meters of limestone covering over 5 million years of deposition near the Cretaceous-Tertiary (K-T) boundary in the Bottaccione Gorge near Gubbio, Italy. Except in 2.6 meters of rock directly adjacent to the huge K-T Ir spike, no Ir anomalies were observed, and the average Ir background was 12.6×10^{-12} gram of Ir per gram of rock (ppt).

Close to the K-T spike of ~ 3000 ppt Ir, there are 7 peaks above and 5 peaks below ranging from 20 to 80 ppt Ir above background. Above the boundary, the Tertiary peaks disappear if ratios are taken with respect to abundance of elements in clay, e.g., Fe, Si, and Al. The curve, which corresponds to carbonate-free measurements, shows essentially a continuous exponential dropoff from a few cm to 1.4 meters above the boundary. The continuous nature of the curve suggests that the source of the Ir was not episodic, i.e., was not due to volcanism. Washing of the continents following the impact of a large asteroid or comet would produce an exponential decrease in Ir abundance in the sediments as a function of time if the Ir available for erosion on the continents decreased by a constant fraction for each unit of time, i.e., the exponential decay of radioactive isotopes.

If the explanation for the Tertiary effects is correct, we would not expect to see the same mechanism in the Cretaceous rock under the K-T spike because Ir obviously could not be washed off the continents before the K-T impact. When ratios are taken to the clay elements for the Cretaceous Ir peaks, they do not disappear as in the Tertiary and, in addition, appear broader and periodic. The Ir tail under the peak is also much smaller than in the Tertiary. We are currently investigating whether diffusion of the iridium downward accompanied by band-

*This work was supported by the Director, Office of Energy Research, Office of Basic Energy Sciences, Engineering and Geosciences Division of the U.S. Department of Energy under Contract No. DE-AC03-76SF00098 and the National Aeronautics and Space Administration Ames Research Center under Contract No. A-71683B and Louisiana State University.

ing, e.g. Liesegang banding of iron in sediments, might explain the Cretaceous peaks.

The peaking of Ir and clay elements in the Tertiary rock (in contrast to the smooth nature of their ratios) may be due to rhythmic dissolution of $CaCO_3$ triggered by the presence of the soft K-T boundary clay between the hard limestone formations. The boundary clay itself is in large part detrital with a component of impact debris (Ir, spherules, and shocked quartz), and we are investigating whether it may be due to pressure dissolution of ~ 10 cm of limestone triggered by the presence of impact debris. The presence of clay is known to encourage pressure dissolution of limestone.

PLANNED ACTIVITIES FOR FY 1988

We will collect, prepare and study about 1100 samples from deep sea cores ODP (Ocean Drilling Project) 689B and 690C taken from the Weddell Sea near Antarctica. The presumed Cretaceous-Tertiary (K-T) boundary regions in these cores have volcanic ash debris, and we want to determine if volcanism accompanied the K-T impact. We will also look for the Late Eocene (conventionally ~ 39.5 million years old) Ir anomaly that we have previously seen only as far south as 36° south latitude. ODP 689B was taken from ~ 64° south latitude. We will look for a Middle Miocene (~ 11.7 million years old) Ir anomaly in the same core which we have so far seen in only one site about 10,000 kilometers away in the Tasman sea.

We will also study a suite of ~ 600 samples (from near and above the 225 million years old Permian-Triassic boundary) collected in China for a Chinese-U.S. cooperative project that we helped organize.

Source Determination of Archaeological Obsidian in Mesoamerica*

F.H. Stross, H.V. Michel, F. Asaro

The neutron activation and the x-ray fluorescence equipment continue to be used for studying trade patterns and their historical implications in Pre-Columbian Central America. Obsidian artifacts, among trade items least affected by time and climate, have been the main objects of our studies in this connection.

*This research was supported by the Council on Research and Creative Work of the University of Colorado, the Quirigua Project of the University of Pennsylvania Museum, The National Science Foundation, the Trent University Research Committee, The National Geographic Society, The University of Texas Institute of Texan Culture, The Department of Sociology and Anthropology at the Southwestern Texas State University, The Social Sciences and Humanities Research Council of Canada, The University of California, Santa Barbara, The Centro Regional de Yucatan of the Instituto Nacional de Antropologia e Historia of Mexico, Mr. & Mrs. Fifield of Milwaukee, Wisconsin, The President's Council of the University of Florida, The Instituto de Antropologia e Historia of Guatemala, The Peabody Museum (Harvard), The Wheelerbrator-Frye Foundation, Mr. Thomas Begel, The University of North Dakota Anthropology General Research Fund and Faculty Research Committees, and the Patrimonio Cultural of El Salvador.

ACCOMPLISHMENTS DURING FY 1987

Careful analytical studies can locate the sources of the raw materials of obsidian artifacts excavated in archaeological sites having access to the volcanic regions in which this natural glass is found. Trade distribution patterns, and their changes with time, can thus be determined; they provide valuable information relating to the history of the regions studied.

Raw materials of obisidian artifacts excavated in Belize, Nicaragua, Honduras, and Costa Rica were found to derive largely from the Guatemalan Highlands, but they included two distinctive groups of unknown origin. The sources of the latter have now been identified and found to be located at La Esperanza and Guinope, both not far from Tegucigalpa. It is remarkable, though unexplained, that although obsidian artifacts from these sources have been found in the regions mentioned above, no artifacts matching the Honduras sources have so far been found in archaeological sites located in the rich Maya centers of Guatemala and Mexico. It is not known if the quality of the obsidian, transportation problem, power-derived monopolies, or other reasons resulted in the uneven distribution of the Honduran obsidian.

While most of the interest in the Maya culture in the past has focused on such rich and spectacular ceremonial sites as Tikal, Palenque, Kaminaljuyu, Yaxchilan, Copan, and their satellites, more recent

projects have dealt increasingly with habitation areas and ports of trade. The latter types of sites may yield less dramatic remains, but more significant information in terms of the daily life of the peoples involved.

The areas studied include inland and off-shore Belize, the Northern Peten, Honduras, Nicaragua and a small island north of Yucatan. The trade distributions shifting with time presumably reflect changes in power structures and other important factors in the history of the Maya. The sites located in the present Belize and the nearby Peten (Guatemala) areas showed distribution patterns foreshadowed in earlier studies: Predominance of the Rio Pixcaya source in the Preclassic periods (before 250 AD) shifted to the El Chayal flow during the Classic (ca 250-900), then to the Ixtepeque source in the terminal Classic and Postclassic (ca 750-1200). These sources are located in the Guatemalan Highlands; very few artifacts derived from Mexico.

Isla Cerritos, just off the northern coast of Yucatan, appears to have been the main port-of-trade for the great site of Chichen Itza in Yucatan. In accord with what is known of the history of this latter site, nearly all of the artifacts found could be dated to relatively late periods, i.e. to terminal Classic and Postclassic. In the suite of artifacts excavated in Isla Cerritos, less than 20% derived from the Guatemalan Highlands, while essentially all of the remaining specimens derived from sources in present-day Mexico. This reflects the presumed incursion of the sites by the Toltecs, who established themselves in Chichen Itza during the period indicated, and left their dramatic mark on that site.

The directors and co-directors of the excavating projects included P. Sheets, F. Lange, K. Hirth, H. McKillop, A. Andrews, W. R. Fowler, P. F. Healy, T. R. Hester, and T. H. Guderjan.

PLANNED ACTIVITIES FOR FY 1988

Interest in Mayan field studies has been shifting toward the southeastern regions of their domain. Pre-Columbian sites in Belize, Honduras, Nicaragua, and Costa Rica recently excavated are furnishing new material on segments of the Maya culture that had not been available so far, and our collaborative research is expected to continue along these lines.

Measurement of Femtogram Quantities of Trace Elements Using an X-ray*

R.D. Giauque, A.C. Thompson, J.H. Underwood, Y. Wu, K.W. Jones [†], and M.L. Rivers [‡]

The development of intense synchrotron radiation beams has led to significant interest in their application for the measurement of trace element concentrations of very small specimens by x-ray fluorescence. Sparks[1] reported the use of an x-ray fluorescence microprobe using synchrotron radiation for the analysis of monazite giant halo inclusions in biotite in the search for superheavy primordial elements. A curved mosaic graphite crystal was employed to both focus and monochromatize the synchrotron radiation beam. Photons of energy 37 keV with a full width at half maximum (FWHM) of 0.4 keV were used. A flux of 15 x 10^{10} photons /(s mm^2) was realized. The actual beam spot size was 0.64 mm^2.

Since 1981 a number of papers have been published regarding the use of x-ray microprobes[2-5]. In most cases, the synchrotron white radiation beam has been collimated using vertical and horizontal slits or doubly curved crystals have been used to focus the radiation. Typical useable beam spot sizes attained are on the order of 700 - 2500 μm^2. More recently Iida and Gohshi[6] have demonstrated the use of a reflection/transmission mirror combination to focus and monochromatize synchrotron radiation. Using an irradiation area of 3500 μm^2, a MDL of 0.03 pg was ascertained for Zn adsorbed on chelate.

*This work was supported by the Office of Energy Research, Office of Health and Environmental Research of the U.S. Department of Energy under contract DE-AC03-76SF00098. The experiment was carried out at the NSLS X-26C beam line which is supported by the Office of Basic Energy Sciences, Chemical Sciences Division, Processes and Techniques Branch of the U.S. Department of Energy Contract No. DE-AC02-76CH00016; the National Institutes of Health as a Biotechnology Research Resource, Grant No. P41RR01838; and the National Science Foundation, Grant No. EAR-8618346.

[†]Brookhaven National Laboratory, Upton, NY 11973

[‡]University of Chicago, Chicago, IL 60637

ACCOMPLISHMENTS DURING FY 1987

The application of an x-ray microprobe that permits very high analytical sensitivities to be realized with improved spatial resolution is described. The instrument permits the spatial distribution measurement of femtogram quantities of trace elements using count intervals of 60 s or less per 10 μm x 10 μm pixel. Calibration of the microprobe was accomplished using National Bureau of Standards thin glass film Standard Reference Materials. A variety of specimens have been scanned to demonstrate the applications that are possible with this microprobe.

The experiments were carried out at the Brookhaven National Synchrotron Light Source (NSLS). White radiation was used as the primary source for the measurements undertaken. The microprobe that was employed to serve as a wide bandpass monochromator and focus the x-ray beam is illustrated in Figure 1. The principal components of the instrument are a pair of concave spherical mirrors coated with tungsten-carbon multilayers. The mirrors are arranged in the Kirkpatrick-Baez geometry. The focusing elements were "super-polished" quartz mirrors with a 6 m concave spherical radius of curvature. Using a dual source sputtering system, each mirror was coated with tungsten-carbon multilayer pairs. The mirror nearest the synchrotron radiation source was coated with 200 multilayer pairs. The second mirror was coated with 100 multilayer pairs. The 2d spacings of the tungsten-carbon multilayer coated mirrors were 58 Å and 87 Å, respectively. The above thicknesses for the multilayer pairs were designed to allow 10 keV radiation to be efficiently reflected when the mirrors were properly aligned. The bandpass of the mirrors was 1 keV and the focused beam spot was less than 10 x 10 μm. A more detailed description of the x-ray microprobe has been reported[7].

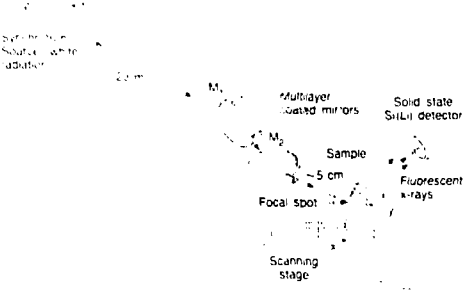

Figure 1. Schematic of the x-ray microprobe. The pair of concave spherical mirrors are coated with tungsten-carbon multilayers. (XBL 876-3046)

Specimens to be scanned were mounted in holders that positioned the specimen at an angle of 45 degrees relative to the incident focused synchrotron radiation beam. A scanning stage allowed the specimen to be translated with respect to the beam spot with step sizes as small as 1 μ in both horizontal and vertical directions. A 5 mm thick, 30 mm^2 Si(Li) detector was aligned so that it was at the beam height and at 90 degrees to the path of the incident radiation. An effective solid angle of $\Omega/4\pi$ = 1.8 x 10^{-3} was viewed by the detector. The synchrotron was operated at 2.5 GeV with a maximum stored electron current of 150 mA. A maximum incident flux of 3 x 10^{9}/s was measured for 10 keV photons in the focused beam spot.

An optical microscope, coupled to a television camera, was used to aid in the positioning of the specimen. Two National Bureau of Standards (NBS) thin glass film Standard Reference Materials, SRM 1832 and 1833 were use to calibrate the system. For our experiments, the reference materials were used to calibrate for the measurement of elements K (Z = 19) through Zn (Z = 30).

Specimens were mounted between two pieces of 6.3 μm polypropylene film that was stretched by a lucite snap ring in a lucite holder. Measurements were made for a single strand of blue green algae cells, freeze-dried thin sections of melanoma tissue from a rat, lung tissue, individual blood red cells, and minute liquid inclusions in laboratory generated quartz specimens.

To establish the minimum detectable limits of the microprobe, x-ray spectral backgrounds were acquired for scattering from air plus two pieces of 6.3 μm polypropylene film. Based on the integrals over the peak locations, Table 1 lists the theoretical (3σ) detection limits ascertained for 60 s live time

Table 1. Minimum Detectable Limits at NSLS

Element	fg/(10 x 10 μm)
K	70
Ca	20
Ti	8
Mn	3
Fe	?
Ni	?
Cu	3
Zn	3

count intervals at a beam current of 150 mA. These very high sensitivity detection limits achieved are applicable for the measurement of trace elements in a thin specimen such as a few biological cells. For biological tissue thin sections of mass thickness 1 mg/cm^2, the minimum detectable limits for these same elements vary between 1 and 40 ppm. For these latter specimens, the intensity of the scattered excitation radiation may be used as a measure of the specimen mass in the beam spot[8] and therefore provide information necessary to determine the concentrations of the elements measured.

As an illustration of the sensitivity of this instrument, a single strand of blue green algae cells was scanned lengthwise in 10 μm steps using count intervals of 30 s per pixel. The size of the individual cells was 3 to 4 μm. Thus, typically three to four cells were in the beam path for each pixel. Figure 2 is a spectrum obtained for one pixel. The elemental quantities listed are in pg. The spectrum clearly shows Mn and Ni at 30 and 20 fg/100 μm^2 level, respectively. The results of an 11 pixel scan along the center of the cell strand are summarized in Figure 3. The initial results obtained clearly demonstrate the high sensitivity and spatial imaging capability of the x-ray microprobe to measure femtogram quantities of specific elements within a 10 x 10 μm beam spot. Additionally, trace element determinations at the ppm concentration level are feasible for thin sections of biological tissues.

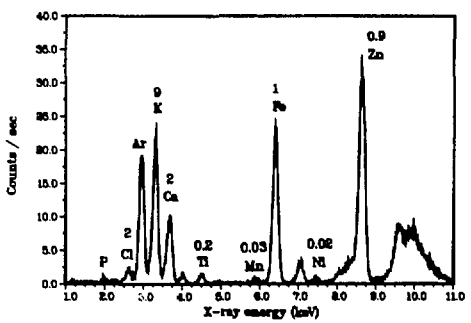

Figure 2. Spectrum obtained in 30 s for a 10 μm x 10 μm pixel of a single strand of blue green algae cells. The element quantities listed above the spectral x-ray lines are in pg. (XBL 876-3045)

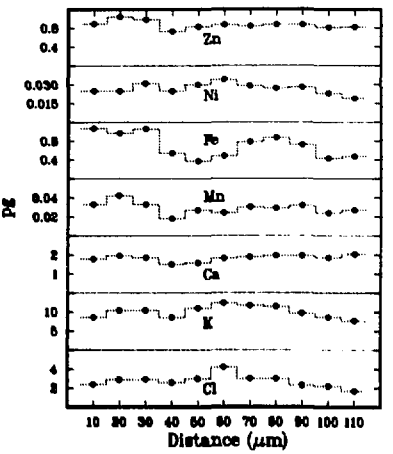

Figure 3. Summary of results ascertained from a scan lengthwise, in 10 μm steps, along the center of a strand of blue green algae cells. (XBL 876-3048)

PLANNED ACTIVITIES FOR FY 1988

Plans are currently being made to fabricate improved mirrors which would give a focused beam spot of a few square microns without any significant loss in x-ray flux. With these mirrors, concentrations of many trace metals in individual biological cells could be ascertained. Such an instrument would be a powerful analytical tool for a variety of research programs. Furthermore, since the specimens are not under vacuum, the x-ray microprobe can accommodate specimens that cannot be studied with an electron microprobe.

REFERENCES

1. Sparks, C.J., Jr. (1980). "Synchrotron Radiation Research," Winick, H. and Doniach, S., Eds.; Plenum Press: New York, p. 459.
2. Jones, K.W., Gordon, B.M., Hanson, A.L., Hastings, J.B., Howells, M.R. and Kraner, H.W. (1984). *Nucl. Instrum. Methods Phys. Res., Sect. B3*, 231, 225.
3. Chen, J.R., Gordon, B.M., Hanson, A.L., Jones, K.W., Kraner, H.W., Chao, E.C.T., and Minkin, J.A. (1984). "Scanning Electron

Microscopy," *SEM, Inc. AMF O'Hare: Chicago, IL, Vol. 4*, p. 1483.

4. Prins, M., Davies, S.T., and Bowen, D.K. (1984), *Nucl. Instrum. Methods Phys. Res., 222*, 324.

5. Prins, M., Kuiper, J.M., and Viegers, M.P.A. (1984), *Nucl. Instrum. Methods Phys. Res., Sect. B3, 231*, 246.

6. Ida, A. and Gohshi, Y. (1985), "Advances in X-ray Analysis," Barrett, C.S. and Predecki, P.K., Eds., Plenum Press New York, No. 28, pp. 61-68.

7. Underwood, J.H., Thompson, A.T., and Wu, Y. *Nucl. Instrum. Methods Phys. Res.*, LBL 24579.

8. Giauque, R.D., Garrett, R.B., and Goda, L.Y. (1979), *Anal. Chem., 51*, 511.